THESIS FOR THE DEGREE OF DOCTOR OF PHILOSOPHY

Optimization, Design, and Analysis of Flexible-Grid Optical Networks with Physical-Layer Constraints

Li Yan

CHALMERS

Communication Systems Group
Department of Electrical Engineering
Chalmers University of Technology

Gothenburg, Sweden 2018

Optimization, Design, and Analysis of Flexible-Grid Optical Networks with Physical-Layer Constraints

Li Yan
ISBN 978-91-7597-763-8

Doktorsavhandlingar vid Chalmers tekniska högskola.
Ny serie Nr 4444
ISSN 0346-718X

This thesis has been prepared using LaTeX.

Communication Systems Group
Department of Electrical Engineering
Chalmers University of Technology
SE-412 96 Göteborg, Sweden
Telephone: + 46 (0)31-772 1865
www.chalmers.se

Printed by Chalmers Reproservice,
Göteborg, Sweden, May 2018.

To my family

Abstract

The theme of this thesis is the optimization, design, and analysis of flexible-grid optical networks that are constrained by physical-layer impairments (PLIs). We consider three flexible-grid network scenarios. The networks in the first class are static nonlinear transparent backbone networks where physical-layer resources are allocated to each traffic demand. The networks in the second class are traffic-variable nonlinear translucent backbone networks where regenerator sites are necessary to recover optical signals from the accumulated noise in long-distance transmission. The third class is data-center networks based on optical spatial division multiplexing. Within each class, our focus is primarily on an efficient and balanced allocation of network resources. Both optimization formulations and heuristic algorithms are proposed for each class. The contributions of this thesis can thus be categorized into three topics, as outlined below.

First, we consider the optimization of network resources in the presence of PLI. The PLI between optical connections is characterized by the Gaussian noise (GN) model and incorporated into resource allocation algorithms. As an example, for a link-level optical communication system, the spectrum usage can be reduced by roughly up to 22% by accurately modelling the PLIs and assigning proper modulation formats and spectrum to optical connections. For resource allocation in the network level, the power spectral density of each optical connection is optimized in addition to the previously mentioned resources.

As a second topic, the design of flexible-grid optical networks is studied. Specifically, we consider the regenerator location problem in traffic-variable translucent backbone networks. Due to the constantly changing traffic, the PLIs suffered by optical connections are also stochastic and, thus, have to be handled from a probabilistic perspective. A statistical network assessment process is used to characterize the noise distributions suffered by optical connections on each link, based on which a heuristic algorithm is proposed to select a set of regenerator sites with the minimum blocking probability.

Finally, we study the trade-off between the blocking probability and total throughput in the modular data center networks (DCNs) based on different optical spatial division multiplexing switching schemes. This performance trade-off is caused by the coexistence of traffic demands with extremely different data rates and number of requests in DCNs. A heuristic resource allocation algorithm is proposed to enable flexible tuning of the objective function and achieve a balanced network performance.

Keywords: Flexible-grid optical network, resource allocation, GN model, DCNs, regenerator location, optimization, heuristic algorithm.

List of Included Publications

The thesis is based on the following appended papers:

[A] L. Yan, E. Agrell, H. Wymeersch, P. Johannisson, R. Di Taranto, and M. Brandt-Pearce, "Link-level resource allocation for flexible-grid nonlinear fiber-optic communication systems," *IEEE Photonics Technology Letters*, vol. 27, no. 12, pp. 1250–1253, Mar. 2015.

[B] L. Yan, E. Agrell, H. Wymeersch, and M. Brandt-Pearce, "Resource allocation for flexible-grid optical networks with nonlinear channel model," (invited paper) *Journal of Optical Communications and Networking*, vol. 7, no. 11, pp. B101–B108, Nov. 2015.

[C] L. Yan, E. Agrell, M. N. Dharmaweera, and H. Wymeersch, "Joint assignment of power, routing, and spectrum in static flexible-grid networks," *IEEE Journal of Lightwave Technology*, vol. 35, no. 10, pp. 1766–1774, Apr. 2017.

[D] L. Yan, Y. Xu, M. Brandt-Pearce, M. N. Dharmaweera, and E. Agrell, "Robust regenerator allocation in nonlinear elastic optical networks with time-varying data rates," submitted to *Journal of Optical Communications and Networking*, Mar. 2018.

[E] L. Yan, M. Fiorani, A. Muhammad, M. Tornatore, E. Agrell, and L. Wosinska, "Network performance trade-off in modular data centers with optical spatial division multiplexing," submitted to *Journal of Optical Communications and Networking*, Feb, 2018.

Other contributions by the author (not included in this thesis):

[F] L. Yan, E. Agrell, and H. Wymeersch, "Resource allocation in nonlinear flexible-grid fiber-optic networks," in *Proc. Optical Fiber Communication Conference (OFC)*, Los Angeles, CA, Mar. 2015, p. Tu2I.5. (top scored)

[G] J. Zhao, L. Yan, H. Wymeersch, and E. Agrell, "Code rate optimization in elastic optical networks," in *Proc. European Conference and Exhibition on Optical Communication (ECOC)*, Valencia, Spain, Sept. 2015, p. We.3.5.1.

[H] L. Yan, J. Zhao, E. Agrell, and H. Wymeersch, "Power optimization in nonlinear flexible-grid optical networks," in *Proc. European Conference and Exhibition on Optical Communication (ECOC)*, Valencia, Spain, Sept. 2015, p. P6.11.

[I] M. N. Dharmaweera, J. Zhao, L. Yan, M. Karlsson, and E. Agrell, "Traffic-grooming- and multipath-routing-enabled impairment-aware elastic optical networks," *Journal of Optical Communications and Networking*, vol. 8, no. 2, pp. 58-70, Jan. 2016.

[J] M. N. Dharmaweera, L. Yan, J. Zhao, M. Karlsson, and E. Agrell, "Regenerator site selection in impairment-aware elastic optical networks," in *Proc. Optical Fiber Communication Conference (OFC),* Anaheim, CA, Mar. 2016, p. Tu3F.1.

[K] L. Yan, E. Agrell, and H. Wymeersch, "Sensitivity comparison of time domain hybrid modulation and rate adaptive coding," in *Proc. Optical Fiber Communication Conference (OFC),* Anaheim, CA, Mar. 2016, p. W1I.3.

[L] M. N. Dharmaweera, L. Yan, M. Karlsson, and E. Agrell, "Nonlinear-impairments- and crosstalk-aware resource allocation schemes for multicore-fiber-based flexgrid networks," in *Proc. European Conference and Exhibition on Optical Communication (ECOC)*, Düsseldorf, Germany, Sept. 2016, p. Th.2.P2.SC6.69.

[M] M. N. Dharmaweera, L. Yan, M. Karlsson, and E. Agrell, "An impairment-aware resource allocation scheme for dynamic elastic optical networks," in *Proc. Optical Fiber Communication Conference (OFC),* Los Angeles, CA, Mar. 2017, p. Th2A.19.

[N] L. Yan, M. Fiorani, A. Muhammad, M. Tornatore, E. Agrell, and L. Wosinska, "Network performance trade-off in optical spatial division multiplexing data centers," in *Proc. Optical Fiber Communication Conference (OFC),* Los Angeles, CA, Mar. 2017, p. W3D.5.

[O] H. Rastegarfar, L. Yan, K. Szczerba, and E. Agrell, "PAM performance analysis in multicast-enabled wavelength-routing data centers," *IEEE Journal of Lightwave Technology*, vol. 35, no. 13, pp. 2569-2579, May 2017.

[P] L. Yan, and E. Agrell, "Capacity scaling of flexible optical networks with nonlinear impairment," (invited paper) in *Proc. International Conference on Transparent Optical Networks (ICTON)*, Girona, Spain, Jul. 2017, p. Th.B4.1.

[Q] L. Yan, Y. Xu, M. Brandt-Pearce, M. N. Dharmaweera, and E. Agrell, "Regenerator site predeployment in nonlinear dynamic flexible-grid networks," in *Proc. European Conference and Exhibition on Optical Communication (ECOC)*, Gothenburg, Sweden, Sept. 2017, p. P2.SC7.43.

[R] L. Yan, Y. Xu, M. Brandt-Pearce, M. N. Dharmaweera, and E. Agrell, "Regenerator allocation in nonlinear elastic optical networks with random data rates," in *Proc. Optical Fiber Communication Conference (OFC),* San Diego, CA, Mar. 2018, p. Th2A.43.

[S] A. Hisham, E. Ström, F. Brännström, and L. Yan, "Scheduling and Power Control for V2V Broadcast Communications with Adjacent Channel Interference," submitted to *IEEE Transactions on Vehicular Technology*, Sept. 2017.

Acknowledgments

First of all, I would like to express my deepest gratitude to my main supervisor Professor Erik Agrell. Erik has been a constant source of support and guidance during my studies. His scientific attitude and curiosity towards optical communications always inspire me in my research. I am also thankful to my cosupervisor Professor Henk Wymeersch for his constant support and encouragement. He can always give me fast and useful feedback in analyzing research problems, presenting results, and writing papers.

I am especially indebted to Professor Maïté Brandt-Pearce for her profound knowledge in optical networks and kind guidance in my research. I benefited tremendously from the discussions with Maïté, which has had a great influence on the direction of my doctoral studies. I had the pleasure to visit Maïté in spring 2017, where we had a fruitful collaboration in the probabilistic modelling of optical networks.

I would like to extend my thanks to friends and colleagues at the Optical Networks Lab at KTH, where I collaborated with many talented people. I specially thank Lena Wosinska for giving me the opportunity to spend three months there, Matteo Fiorani for introducing me to the optical data center networks, and Ajmal Muhammad for the patient guidance in optimization.

Thanks to my colleagues in our group, in alphabetical order: Àlex, Alireza, Andreas, Anver, Árni, Bile, Chao, Christopher, Christian, Cristian, Erik, Fredrik, Fuxi, Gabo, Guido, Hao, Houman, Jesper, Johan, Juzi, Kamran, Kathi, Keerthi, Lotfollah, Markus, Misha, Mohammad, Morteza, Naga, Nil, Rahul, Rajet, Reza, Rocco, Roman, Sven, and Ulf. Many thanks to Erik Ström for his dedication in creating an inspiring research group and the administrative staff for making a fantastic and stimulating work environment. I would also like to thank all my colleagues from MC2 part at the fiber optics communication research center (FORCE) for creating the unique and diverse research environment.

Last but not least, my deepest gratitude goes to my parents and family for the endless support.

Li Yan
Gothenburg, May 2018

This work was funded in part by the Swedish Research Council (VR) under grants no. 2012-5280, 2014-6138, and 2013-5271, and by the Swedish Foundation for Strategic Research (SSF) via grant no. RE07-0026. I would also like to thank Ericsson's Research Foundation for sponsoring my research visit to University of Virginia.

Acronyms

ASE:	Amplified spontaneous noise
BER:	Bit error rate
BPSK:	Binary phase shift keying
BV-WXC:	Bandwidth-variable wavelength crossconnect
BV-T:	Bandwidth-variable transceiver
CL:	Connection list
CUT:	Channel under test
DAC:	Digital-to-analog converter
DC:	Data center
DCN:	Data center network
DSP:	Digital signal processing
EDFA:	Erbium-doped fiber amplifier
FEC:	Forward error correction
GN:	Gaussian noise
GN-RMSA:	Gaussian noise model based routing, modulation format, and spectrum assignment
ILP:	Integer linear programming
LOGO:	Local optimum global optimum
LOGON:	Local optimum global optimum Nyquist
LPC:	large port count
MCI:	Multiconnection interference
MDC:	Modular data center
MILP:	Mixed integer linear programming

MINLP:	Mixed integer nonlinear programming
NLI:	Nonlinear interference
NLS:	Nonlinear Schrödinger
O-E-O:	optical-electrical-optical
OSNR:	Optical signal to noise ratio
PDL:	Polarization-dependent loss
POD:	Performance optimized DC
PLI:	Physical layer impairment
PM:	Polarization multiplexing
PMD:	polarization-mode dispersion
PSD:	Power spectral density
QAM:	Quadrature amplitude modulation
QoT:	Quality of transmission
QPSK:	Quadrature phase shift keying
RLP:	Regenerator location problem
RMSA:	Routing, modulation format, and spectrum assignment
RS:	Regenerator site
RSA:	Routing and spectrum assignment
RWA:	Routing and wavelength assignment
SCI:	Selfconnection interference
SDM:	Spatial division multiplexing
SNR:	Signal to noise ratio
ToR:	Top of Rack
TR:	Transmission reach
WDM:	Wavelength division multiplexing
XCI:	Crossconnection interference

Contents

Part I

Overview

Chapter 1

Introduction

Being the foundation of today's information society, the fiber-optical communication networks were first invented in the 1970s and since then gradually revolutionized the world by connecting everything easier and faster. Thanks to the extremely high bandwidth and long transmission distances, optical networks have been an enabling technology for Internet, data centers, and various communication networks. The enormous growth of these applications, in turn, drives the development of optical networks toward greater efficiency and flexibility [1]. Meanwhile, numerous techniques have been innovated to improve the performance of optical communications [2].

Nowadays, wavelength division multiplexing (WDM) is commonly used in regional and backbone optical networks to modulate signals onto wavelengths and transmit through fibers [3]. These wavelengths are located on predetermined wavelength grids, which divide the optical spectrum into fixed 50 GHz spectrum slots [4] carrying fixed data rates[1]. Due to the exponentially growing network traffic demands, the data rates increase from 10 Gbps to 100 Gbps and beyond [2]. The growth of bit rate per wavelength requires higher order modulation formats and larger bandwidths. However, current optical networks cannot support this constant capacity increase due to the fixed spectrum grids. To properly address this challenge, more flexible networks are considered [3], which combine adaptive and intelligent hardware to enable new flexible-grid optical networks.

In flexible-grid optical networks, variable bandwidth and high throughput are enabled by adaptive transceivers and various new network features [6, 7]. In the spectrum domain, optical connections will be no longer situated in the fixed 50 GHz spectrum slots, but rather at finner-granular grids or even gridless frequencies based on their different requirements, transmission distances, and network conditions. In the spatial domain, optical spatial division multiplexing (SDM) enabled by multicore, multimode, or multielement fibers can be used as a cost-effective and energy-efficient solution to ultimately boost the capacity of optical communications. Furthermore, enabled by bandwidth-variable wavelength crossconnects (BV-WXCs) and bandwdth-variable transceivers (BV-Ts), the network operators will be able to dynamically change the bandwidths of optical connec-

[1] In some optical networks, the data rate per wavelength can be chosen from a set of available rates, e.g., 10, 40, or 100 Gbps [5].

tions according to real-time communication requirements and, thus, achieve cost-effective and highly available connectivity services in a traffic-variable network scenario [8].

To fully exploit the advantages provided by the flexible-grid optical networks, resource allocation algorithms that achieve efficient spectrum utilization and a balance between different figures of merit are desirable. Moreover, the resource allocation algorithms should also fulfill the requirements of all the communication requests in terms of both data rate and quality of transmission (QoT). However, due to the heterogeneous allocations of modulation formats and optical power spectral densities (PSDs), the generation of physical-layer impairments (PLIs) is extremely complicated and relatively hard to estimate. Therefore, an accurate and computationally efficient channel model is necessary in resource allocation algorithms.

Traditionally, PLIs in the optical networks are estimated by the transmission reach (TR) method, which is the worst-case transmission distance of a transmission scheme in fully loaded spectrum. This approach overprovisions the signal-to-noise ratio (SNR) margins such that all the channels have acceptable QoTs in any network condition. However, this results in a waste of network resources in most of the cases. As a more recent method, the Gaussian noise (GN) model is proposed to characterize the nonlinear signal distortions in dispersion-uncompensated optical fibers with reasonable accuracy and low computational complexity [9–14]. Based on perturbation analysis, the GN model finds an approximate analytical solution to the nonlinear propagation equation, where the nonlinear interference (NLI) behaves as stationary additive Gaussian noise [12].

In [Paper A–C], we precisely predict SNRs and, thus, QoTs of all the channels with the GN model, based on which the physical-layer resources are optimized. Specifically, in [Paper A], the link level resource allocation is optimized to reduce the spectrum usage by around 20% in comparison with the TR model based resource allocation. In [Paper B], the resource allocation algorithm proposed in [Paper A] is generalized to the network level by assuming precalculated routes and orders of traffic demands in the spectrum domain. In [Paper C], a joint optimization of power spectral density (PSD), routing, and spectrum is carried out to mitigate PLIs and achieve efficient resource utilization.

Despite accurate PLI estimation and optimized resource allocation, accumulated impairments in some long-haul backbone networks can still be higher than the maximum tolerable noise of chosen modulation formats. Therefore, one or more optoelectronic regenerators have to be used to restore optical signals. Each regenerator adds a cost comparable to a pair of endpoint transceivers [15] and, thus, requires system operators to predeploy them as efficiently as possible. By deploying regenerators at a subset of the network nodes, referred to as regenerator sites (RSs), we can achieve better sharing of spare regenerators from randomly variable demands and improved operational efficiency with fewer truck rolls [16], which require system operators to dispatch technicians in a truck to install or maintain the network equipment.

The problem of allocating a minimum set of RSs is the regenerator location problem (RLP) [15]. Previous studies have investigated the RLP in single-line rate or waveband-switched WDM networks from cost and energy consumption perspectives [15–19]. Efficient heuristic algorithms have also been proposed to find RSs in mixed-line rate WDM networks [20, 21]. However, these researches either assume detailed PLIs as known system parameters [17, 18], or rely on the TR model [15, 16, 20, 21], which represents the

impairments as reachability in the worst case with fiber links fully loaded.

In the traffic-variable network scenario, which is enabled by BV-WXCs and BV-Ts, the data rates of each traffic request is constantly changing as functions of time. Consequently, the PLIs generated in the network are also random variables and the solution of the RLP should be robust to this PLI variance. To this end, in [Paper D] we characterize the probability distributions of PLIs on each link of the network statistically and optimize the RS locations with respect to blocking probabilities.

Besides the regional and backbone optical networks, the flexible-grid optical networks can also be employed in other applications. One of these examples is to boost the throughput of modular data center (MDC) networks with spatial division multiplexing (SDM) [22], which can also be combined with flexible grid to achieve even higher capacity [7, 23]. Depending on whether optical signals on different spectral and spatial elements are coupled to form superchannels, several SDM switching schemes with different levels of flexibility and complexity have been investigated [7, 23, 24].

Current state-of-the-art resource allocation algorithms in SDM networks focus either on the maximization of throughput or minimization of blocking probability. However, they are not suitable in the data center network (DCN) application where the distributions of data rates and number of demands are highly unbalanced. Previous studies [25–28] have revealed that the majority of flows within the DCNs have low data rates (referred to as mice flows), yet a large part of total throughput belongs to a few huge traffic flows (referred to as elephant flows). This unbalance becomes more severe when demands are aggregated in MDCs, where the contrast between different flow classes is even stronger. Consequently, targeting the minimization of the blocking probability may incur high blocking of bandwidth-intensive elephant connections and hence reduce the network throughput. On the other hand, maximizing the throughput may lead to blocking of an excessive number of mice flows. Therefore, a balance between the blocking probability and throughput should be sought to guarantee fairness and efficiency in DCNs. In [Paper E], we have investigated the relation between different figures of merit in SDM-based MDCs and quantified the trade-off between the blocking probability and throughput.

The format of this thesis is a so-called *collection of papers*. It is divided into two parts, where Part I serves as an introduction to Part II consisting of the appended papers. The remainder of Part I is structured as follows. Chapter 2 provides an introduction to optical fiber communications and its different physical-layer impairment models. In Chapter 3, we give a brief introduction to resource allocation in static transparent optical networks. In Chapter 4, we review some basic background about the regenerator location problem. The optical data center networks are discussed in Chapter 5.

The following notation is used in the introductory part of the thesis.

- $\mathbb{R}, \mathbb{R}_+$, $\mathbb{Z}_+$, and $\mathbb{B}$ denote the sets of real numbers, nonnegative real numbers, nonnegative integers, and $\{0, 1\}$, respectively.
- The cardinality of a set A is denoted by $|A|$.

The meaning of all symbols is consistent within each chapter but may be inconsistent across the thesis due to the many variables involved in some of the optimization formulations.

Chapter 2

Physical-Layer Impairments and Modelling

The performance and total costs of optical communication are ultimately determined by impairments imposed by various elements along optical transmission systems. These impairments originate from electrical devices, optical components, and transmission medium. The electrical devices and optical components are mostly fixed at the deployment stage, whereas parameters related to transmission in optical fibers are still adjustable in the operation of flexible-grid optical networks. Consequently, it is crucial to understand the impairments caused by optical fibers to improve the overall network efficiency.

In this chapter, we first overview system impairments of optical transmission systems in Section 2.1. The rest of the chapter is dedicated to impairments of optical channels. Specifically, in Section 2.2, the nonlinear Schrödinger (NLS) equation is introduced. In Section 2.3, the chromatic dispersion in optical fiber is discussed. The optical amplification and its corresponding noise is described in Section 2.4. In Section 2.5, the NLIs generated by copropagating optical connections are reviewed. Different models measuring NLIs are introduced in Section 2.6. Finally, the requirement of QoT is described in Section 2.7.

2.1 System Impairments

As illustrated in Figure 2.1, there are three main building blocks in optical communication systems: a transmitter, an optical channel, and a receiver. The transmitter converts electrical input to optical signals, which propagate through the channel to the receiver. Each of the building block can introduce various kind of signal degradations that will impact the system performance negatively.

Inside a transmitter, the digital input is first converted to analog signal by digital-to-analog converter (DAC) and then amplified and modulated onto lightwave generated by semiconductor lasers. All these components contribute to the signal degradation

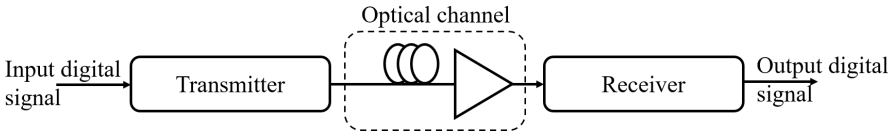

Figure 2.1: Generic optical communication system.

of a transmitter. The laser generates phase noise due to its finite line width. The amplitude resolution of the DAC limits the generation of high-order modulation formats. The nonlinear behavior of the microwave amplifier and modulator can introduce signal distortions. The modulator is also affected by finite extinction ratio and I/Q imbalance, which do not introduce much penalty for low-order modulation formats but can be an issue for higher-order schemes such as 64-ary quadrature amplitude modulation (QAM).

The optical channel is affected by impairments introduced by different components along the link. The optical fiber contributes to the chromatic dispersion, polarization-mode dispersion (PMD), polarization-dependent loss (PDL), and nonlinear effects. The erbium-doped fiber amplifier (EDFA) can accumulate white Gaussian noise. And the cascade of filters in wavelength-selective switches at optical nodes causes signal distortion in the spectrum domain. These impairments are closely related to route, spectrum, and PSD assigned to optical connections.

At the receiver side, the impairments of hardware is less problematic compared to the transmitter [29, p. 90]. Limitations of bandwidth, amplitude resolution, and SNR are introduced by the local oscillator laser, analog-to-digital converter, and photodetector.

Some of the signal distortions introduced by transmitters and receivers (e.g., bandwidth limitations and nonlinear effects of components) can be tackled by proper digital signal processing (DSP) techniques, whereas others (e.g., the effective number of bits in DAC and extinction ratio) are hard to compensate for and can only be considered by the predefined system margins [30]. The channel impairments, however, are closely related to the transmission parameters assigned to each connection and can be mitigated by appropriate resource allocation. Therefore, in the following of the thesis, we are mainly concerned with the physical impairments introduced by optical fibers. Moreover, we will only consider the most significant impairments, which will be elaborated in the following sections. Other impairments such as PMD and PDL can be mitigated by receiver DSPs and are not discussed in this thesis.

2.2 Waveform Propagation in Optical Fibers

The single-polarization waveform-propagation equation in an optical fiber is modeled using the NLS equation with loss [31, p. 40]

$$\frac{\partial A}{\partial z} = i\gamma|A|^2 A - i\frac{\beta_2}{2}\frac{\partial^2 A}{\partial t^2} - \frac{\alpha}{2}A, \tag{2.1}$$

where $A = A(z,t)$ is the slowly varying complex envelope of the optical field, z is the distance of propagation, γ is the nonlinear coefficient of the fiber, $|A|^2$ is the power of the optical envelope, β_2 is the group velocity dispersion coefficient, α is the power attenuation factor of the fiber, and t is the time coordinate in a reference frame moving with the optical envelope. To have physical meaning, here we assume that $|A|^2$ is finite. Given an initial envelope $A(0,t)$ at the input of a fiber, (2.1) tells us the propagated waveform envelope at any distance z in the fiber.

The three terms at the right-hand side of (2.1) govern, respectively, the effects of nonlinearity, dispersion, and fiber losses on optical waveforms. In the following sections, we introduce these impairments in detail.

2.3 Chromatic Dispersion

In a dispersive medium the group velocities[1] of different wavelengths are different. This phenomenon is called group velocity dispersion or chromatic dispersion. In long-haul optical communication systems, the accumulated chromatic dispersion is large enough to broaden the waveform width in the time domain and thus leads to inter-symbol interference.

To study the waveform propagating in a linear dispersive medium, we can neglect the nonlinearity and power losses by setting the nonlinear coefficient $\gamma = 0$ and the power attenuation factor $\alpha = 0$. The NLS equation thus becomes

$$\frac{\partial A}{\partial z} = -i\frac{\beta_2}{2}\frac{\partial^2 A}{\partial t^2}. \tag{2.2}$$

The closed-form solution of (2.2) in the spectrum domain is

$$\tilde{A}(z,\omega) = \tilde{A}(0,\omega)\exp(i\beta_2\omega^2 z/2), \tag{2.3}$$

where $\tilde{A}(z,\omega)$ is the Fourier transform of the time domain waveform envelope $A(z,t)$. From (2.3) we know that the chromatic dispersion can be modeled as a linear all-pass filter. The amplitude of the waveform frequency is unaffected, but a frequency-dependent phase shift is introduced.

Traditionally, chromatic dispersion is compensated for in the optical domain by a dispersion-compensating fiber or a fiber Bragg grating. The dispersion-compensating fiber has the opposite sign of β_2 compared to the single-mode fiber. The fiber Bragg grating reflects different frequency components of the chirped optical waveform at different positions in the fiber grating to compress the waveforms. In modern high speed coherent transmission systems, chromatic dispersion is compensated for by digital filters in the receiver. This DSP technique avoids additional nonlinearities or losses induced by the optical compensation modules, and enables more flexible deployment of fibers. In the rest of this thesis, we assume that the chromatic dispersion is tackled by receiver DSP and no optical dispersion compensation is present in the fiber link.

[1] Group velocity measures the velocity at which energy or information is conveyed along an optical waveform.

2.4 Optical Amplification and Noise

The power loss of optical signals inside a fiber comes from sources such as Rayleigh scattering, material absorption, bending of the fiber, and scattering of light at the core-cladding interface [31, pp. 5–6]. The fiber loss can be described mathematically by ignoring the dispersion and nonlinearity in (2.1) as

$$\frac{\partial A}{\partial z} = -\frac{\alpha}{2}A. \tag{2.4}$$

The solution of (2.4) is

$$A(z,t) = A(0,t)\exp\left[-\alpha z/2\right]. \tag{2.5}$$

Equation (2.5) shows that the waveform amplitude decreases exponentially as a function of the propagation distance z. If $P_0 = \int_{-\infty}^{\infty} |A(0,t)|^2 dt$ is the power of the optical signal at the input of a fiber with length of L, the received power P_R is given by

$$P_R = P_0 \exp(-\alpha L). \tag{2.6}$$

The attenuation constant α is a measure of total fiber losses in linear scale. It is customary to express α in unit of dB/km using the relation

$$\alpha_{\text{dB}} = -\frac{10}{L}\log_{10}\left(\frac{P_R}{P_0}\right) = 4.343\alpha. \tag{2.7}$$

In commercial optical communication systems, fibers usually exhibit a loss around 0.2 dB/km, which means that after the transmission of a fiber span (usually around 100 km) the optical power is attenuated by more than 20 dB and well below the sensitivity threshold of photodetectors in the receiver. Consequently, in long-haul transmission, amplifiers are necessary to boost the intensity of optical signals periodically at the end of fiber spans. The EDFA is the most commonly used amplifier in optical communication systems.

Commercial amplifiers can induce ASE noise to optical signals, which is intrinsic to EDFAs [32, pp. 255–256] and can be modeled as additive white Gaussian noise with the PSD per span per polarization as

$$G_{\text{span}}^{\text{ASE}} = (e^{\alpha L} - 1)h\nu n_{\text{sp}}, \tag{2.8}$$

where h is the Planck constant, ν is the light frequency, and n_{sp} is the spontaneous emission factor. The ASE noise can interact with other impairments in the fiber to deteriorate the signal quality.

Commercial EDFAs usually have a flat gain spectrum such that different wavelengths can experience the same gain [32, pp. 258–259]. Consequently, as long as the EDFA is not saturated, connections with different input PSDs will keep the PSD difference (in dB) after the amplification.

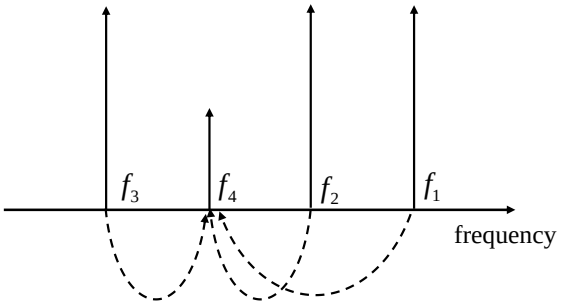

Figure 2.2: Four-wave mixing generates new frequency component f_4 from three existing frequencies f_1, f_2 and f_3.

2.5 Nonlinear Interference

The nonlinear effects in an optical fiber originate from nonlinear refraction, a phenomenon referring to the intensity dependence of the refractive index. In the presence of the optical field, the refractive index of the fiber is slightly changed. This varied refractive index further changes the phase of optical signal and results in NLIs affecting QoTs.

Specifically, the fiber nonlinearity can be understood by ignoring the dispersion and power loss in (2.1) as

$$\frac{\partial A}{\partial z} = i\gamma |A|^2 A. \tag{2.9}$$

The solution of (2.9) is

$$A(z,t) = A(0,t) \exp\left[i\gamma |A(0,t)|^2 z\right]. \tag{2.10}$$

Equation (2.10) describes the nonlinear distortion in the presence of one waveform modulated on a single wavelength, where the signal phase is changed proportionally to the signal power $|A(0,t)|^2$. In WDM and flexible-grid optical networks, signals from multiple connections with different wavelengths may overlap in the time domain and lead to more complex interference like four-wave mixing, where interactions between three existing wavelengths produce a fourth wavelength [31, pp. 369–370]. An illustration of four-wave mixing is shown in Figure 2.2.

In the spectrum domain, the nonlinear effects can be classified into three categories according to their origins: selfconnection interference (SCI), crossconnection interference (XCI), and multiconnection interference (MCI). As is shown in Figure 2.3, for a specific connection, its SCI is the interference generated by the connection to itself. The XCI of the connection comes from its interaction with another connection. Its MCI is produced by at least two other connections outside the affected connection. In a dispersion uncompensated transmission system, SCI and XCI are the dominant NLIs, while the relative strength of MCI is almost always negligible [12].

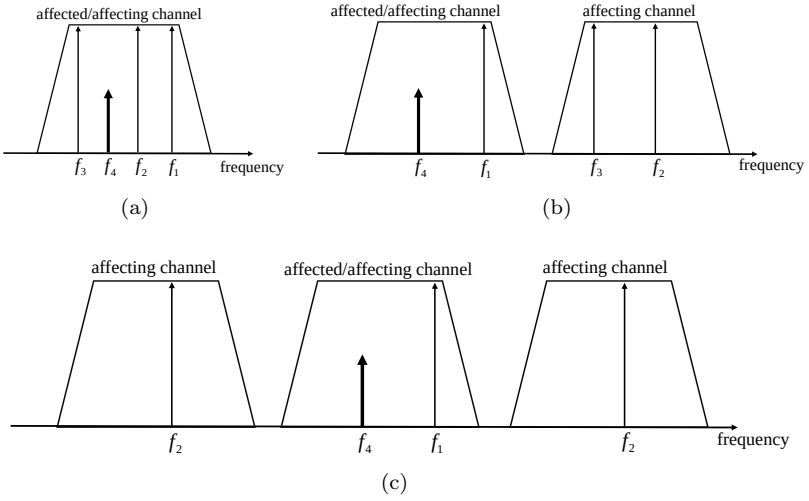

Figure 2.3: Classification of NLI. Thin tall arrows (f_1, f_2, and f_3): generating frequency components. Thick short arrow (f_4): generated frequency component. (a): SCI, connection is affected by itself; (b): XCI, connection is affected by the interaction between itself and another connection; (c): MCI, at least two affecting connections outside the affected connection are involved.

Unlike the chromatic dispersion that is equivalent to a linear all-pass filter, the nonlinear effects generate new frequencies in the spectrum domain. The new frequency component can interfere with other existing wavelengths and degrade QoTs of copropagating connections. Moreover, the nonlinear effects can further interact with chromatic dispersion and ASE noise to generate complicated nonlinear phase and amplitude noise, which is hard to capture analytically. Actually, nonlinearity is a serious problem limiting the efficiency of optical transmission systems.

Nonlinearities can be partly compensated for by digital backpropagation, which solves the inverse NLS equation by simulating the received signal with reversed parameters $(-\beta_2, -\gamma, -\alpha)$ [33–35]. In this thesis, we assume that the SCI is compensated for by digital backpropagation for the resource allocation algorithm in [Paper B] to facilitate its comparison with the benchmark [36]. However, this can be easily extended to the SCI-uncompensated scenario by modifying the NLI estimation as in [Paper A] and [Paper C–D].

2.6 Modelling of PLIs

The TR and GN models are two widely used methods to estimate PLIs and guarantee satisfactory QoTs. The TR model has been applied in the WDM networks due to its simplicity and effectiveness in homogeneous network conditions, where all the connections

have the same transmission parameters and locate on uniform spectrum grids. On the other hand, the GN model is an analytical model that takes transmission parameters of all the connections as inputs and calculates the NLI noise.

In the TR model, the reach is defined as the distance that an optical connection can travel before its QoT degrade to an unacceptable level. Many factors affect the maximum reach an optical connection can transmit: the launched power, modulation format, bit rate, interference from other connections, etc. [37]. To guarantee a robust PLI estimation under all network conditions, the TR is usually measured in the worst case scenario, where the connection under test is located in the middle of a fully loaded spectrum. Typically, the TR is a function of given bit rate and modulation format [38].

Due to the conservative nature of the TR model, it is very likely that a connection in the network can transmit much longer than its TR. This overestimation of PLIs causes unnecessary overprovision of network resources and affects the network utilization and efficiency negatively. To overcome this disadvantage, the GN model was proposed to estimate the PLIs more accurately. In the GN model, the NLI noise suffered by an optical connection is modelled as additive Gaussian noise under the following assumptions [9, 10]:

1. a coherent polarization-multiplexed (PM) system without optical compensation for chromatic dispersion;
2. the transmitted signal PSD is equal in both polarizations for each connection;
3. the connection spectrum is rectangular and does not overlap with other connections;
4. the NLI generated in different fiber spans sums incoherently over the whole link;
5. the losses of each span are compensated for by an EDFA at the end of the span;
6. all spans are long enough;
7. the MCI is neglected due to its negligible strength.

Under the above-mentioned assumptions, by applying perturbation analysis and approximations to the waveform-propagation equation, the NLI PSD per span per polarization for connection i can be expressed as [9]

$$G_i^{\mathrm{NLI}} = G_i^{\mathrm{SCI}} + G_i^{\mathrm{XCI}} \tag{2.11}$$

where

$$G_i^{\mathrm{SCI}} = \frac{3\gamma^2}{\alpha^2} F_{ii}^2 G_i^3, \quad G_i^{\mathrm{XCI}} = \frac{6\gamma^2}{\alpha^2} G_i \sum_{\substack{j \in D \\ j \neq i}} F_{ij}^2 G_j^2. \tag{2.12}$$

Here D is the set of connections in the network. G_i^{SCI} and G_i^{XCI} are the SCI and XCI PSDs per span per polarization of connection i, respectively. G_i is the transmitted PSD per polarization for connection i. F_{ij}^2 for $i, j \in D$ is the NLI efficiency function

representing the NLI strength:

$$\begin{aligned} F_{ij}^2 =& \frac{2}{\xi}\Bigg\{ \operatorname{Im}\operatorname{Li}_2\left[\sqrt{-1}\frac{\Delta f_i}{2}\left(f_i - f_j + \frac{\Delta f_j}{2}\right)\xi\right] \\ &+ \operatorname{Im}\operatorname{Li}_2\left[\sqrt{-1}\frac{\Delta f_i}{2}\left(f_j - f_i + \frac{\Delta f_j}{2}\right)\xi\right]\Bigg\}, \end{aligned} \tag{2.13}$$

with

$$\xi = \frac{4\pi^2|\beta_2|}{\alpha}, \tag{2.14}$$

and Li_2 is the dilog function. f_i and Δf_i are the carrier frequency and bandwidth of connection i for $i \in D$, respectively.

The dilog function in (2.13) can be simplified using its asymptotic expansion. As a result, the NLI efficiency function F_{ij}^2 for $i, j \in D$ can be approximated by the hyperbolic arcsin function if $i = j$ [14], and the logarithm function if $i \neq j$ [9]

$$\begin{aligned} F_{ii}^2 &\approx \frac{\alpha}{2\pi|\beta_2|}\operatorname{arcsinh}\left(\frac{\pi^2|\beta_2|}{2\alpha}\Delta f_i^2\right), \\ F_{ij}^2 &\approx \frac{\alpha}{4\pi|\beta_2|}\log\left|\frac{|f_i - f_j| + \Delta f_j/2}{|f_i - f_j| - \Delta f_j/2}\right|, i \neq j. \end{aligned} \tag{2.15}$$

The hyperbolic arcsin function is used for the SCI coefficient F_{ii}^2 as it approximates the dilog function better than the logarithm function when $\pi^2|\beta_2|\Delta f_i^2/2\alpha \ll 1$, in which case the logarithm function tends toward negative infinity. On the contrary, the argument of the XCI coefficient F_{ij}^2 in (2.15) is always greater than 1 and, thus, the logarithm function gives acceptable approximation error.

From (2.11), (2.12), and (2.15), the NLI PSD per span per polarization is

$$\begin{aligned} G_i^{\mathrm{NLI}} =& \frac{3\gamma^2}{2\pi\alpha|\beta_2|}G_i\Bigg(G_i^2\operatorname{arcsinh}\left(\frac{\pi^2|\beta_2|}{2\alpha}\Delta f_i^2\right) \\ &+ \sum_{\substack{j\in D \\ j\neq i}} G_j^2\log\left|\frac{|f_i - f_j| + \Delta f_j/2}{|f_i - f_j| - \Delta f_j/2}\right|\Bigg). \end{aligned} \tag{2.16}$$

Since we have assumed that NLI from different spans are accumulated incoherently, (2.16) can be readily extended to a network of multiple spans and links as

$$\begin{aligned} G_i^{\mathrm{NLI}} =& \frac{3\gamma^2}{2\pi\alpha|\beta_2|}G_i\Bigg(G_i^2 N_i^{\mathrm{s}}\operatorname{arcsinh}\left(\frac{\pi^2|\beta_2|}{2\alpha}\Delta f_i^2\right) \\ &+ \sum_{\substack{j\in D \\ j\neq i}} G_j^2 N_{ij}^{\mathrm{s}}\log\left|\frac{|f_i - f_j| + \Delta f_j/2}{|f_i - f_j| - \Delta f_j/2}\right|\Bigg), \end{aligned} \tag{2.17}$$

Table 2.1: The available modulation formats, their SEs, and linear scale SNR thresholds $\mathrm{SNR}^{\mathrm{th}}(c)$ to achieve a preFEC BER of 4×10^{-3}.

Modulation Format	c (bit/s/Hz)	$\mathrm{SNR}^{\mathrm{th}}(c)$
PM-BPSK	2	3.52
PM-QPSK	4	7.03
PM-8QAM	6	17.59
PM-16QAM	8	32.60
PM-32QAM	10	64.91
PM-64QAM	12	127.51

where N_i^{s} is the number of spans traversed by connection i, and N_{ij}^{s} is the number of spans shared by connections i and j (N_{ij}^{s} equals 0 if i and j do not share any link). Notice that the NLI PSD is independent of fiber span length since we have assumed that all spans are long enough to have the same effective length[2].

It follows from (2.17) that the NLI PSD of one connection depends on the routes and transmission parameters of all the connections in optical networks. Therefore, a global knowledge of all the resources allocated in the network is required to estimate the NLI, implying a centralized network planning strategy [9]. For example, resource allocation algorithms in both link [Paper A] and network levels [Paper B] are studied, which outperform their TR-based counterparts significantly in flexible-grid optical networks.

2.7 Quality of Transmission

The GN model can be used to estimate QoTs, which is specified by the BER of each connection at the receiver side after forward error correction (FEC) decoding (i.e., postFEC BER). In this thesis, we assume hard decision FEC decoding and fixed code type and code rate for all the connections in the network. Therefore, the postFEC BER can be calculated given the BER before the FEC decoder (i.e., preFEC BER), which is further related to the SNR of the received signal. To guarantee a satisfactory QoT, the actual SNR should be no less than a certain SNR threshold that is determined by the selected modulation format and FEC code type and code rate. On the other hand, the actual SNR of connection i can be estimated by

$$\mathrm{SNR}_{\mathrm{Rx},i} = \frac{G_i}{G_{\mathrm{Rx},i}^{\mathrm{ASE}} + G_{\mathrm{Rx},i}^{\mathrm{NLI}}}, \tag{2.18}$$

where G_i is the transmitted PSD per polarization, $G_{\mathrm{Rx},i}^{\mathrm{ASE}} = G_i^{\mathrm{ASE}} N_i^{\mathrm{s}}$ is the accumulated ASE noise along the fiber links traversed by connection i, G_i^{ASE} is the ASE noise per span per polarization in (2.8), and $G_{\mathrm{Rx},i}^{\mathrm{NLI}}$ is the NLI PSD given by the GN model in (2.17). The requirement for acceptable QoT is hence translated to an inequality constraint on

[2]The effective length $L_{\mathrm{eff}} = [1 - \exp(-\alpha L)]/\alpha$ is the length over which the optical power remains large enough for nonnegligible nonlinear effects.

SNR

$$\mathrm{SNR}_{\mathrm{Rx},i} \geq \mathrm{SNR}_i^{\mathrm{th}}, \tag{2.19}$$

where $\mathrm{SNR}_i^{\mathrm{th}}$ is the SNR threshold of connection i.

According to (2.19), the SNR threshold is the minimum SNR achieving a certain preFEC BER requirement. The set of available modulation formats in this work is PM binary phase shift keying (BPSK), PM quadrature phase keying shift (QPSK), PM-8QAM, PM-16QAM, PM-32QAM, and PM-64QAM. The spectral efficiencies (SEs) are denoted by c and listed in Table 2.1. Since the modulation formats in Table 2.1 have distinct SEs, we can use c to denote them as well. The SNR thresholds of these modulation formats with Gray mapping [39, 40], $\mathrm{SNR}^{\mathrm{th}}(c)$, are also listed in Table 2.1. Note that it is possible to use a subset of the available modulation formats, and the preFEC BER requirement may change according to specific requirement[3].

[3]Here, the preFEC BER threshold of 4×10^{-3} is chosen to be the same as the benchmark [36] of our proposed resource allocation algorithms to facilitate numerical comparisons.

Chapter 3

Resource Allocation in Static Transparent Networks

Network resource allocation is considered as one of the key elements in flexible-grid optical networks. It assigns appropriate resources to different traffic demands to realize satisfactory QoTs and efficient resource usage. In this chapter, we review some basic concepts behind network resource allocation algorithms in static transparent optical networks. In this network scenario, the traffic demands are assumed static and known in advance, and the resource allocation is performed offline. Additionally, we are concerned with transparent networks where signal regeneration is not employed.

We start by giving an overview of the optical networks in Section 3.1. The classic routing and wavelength assignment (RWA) problem in fixed-grid WDM networks is introduced in Section 3.2. In Section 3.3, we review the routing and spectrum assignment (RSA) problem based on the TR model, which is the counterpart of the RWA problem in flexible-grid optical networks. In Section 3.4, the routing, modulation format, and spectrum assignment (RMSA) in problem flexible-grid networks based on the TR model is discussed. The RMSA problem based on the GN model is introduced in Section 3.5. Finally, power optimization based on the GN model is briefly introduced in Section 3.6.

3.1 Overview of Optical Networks

According to the geographic extent, optical networks can be briefly categorized into three types: access, metro, and backbone networks [41, p. 3]. Access networks span a few kilometers and serve hundreds to thousands of customers. The traffic in access networks are aggregated by metro networks, which typically interconnect a number of access networks within a range of hundreds to thousands of kilometers. At the top of the hierarchy, multiple metro networks are interconnected via backbone networks. A backbone network carries traffic across multiple metro networks and is shared among millions of customers or even more. The geographic range of a backbone network is typically a few thousands of kilometers.

As the network moves closer to customers, its cost is amortized over fewer end users and, thus, the network becomes more cost sensitive. Therefore, it is common to deploy new technologies in backbone networks first. As the technology achieves a lower price, it gradually extends closer towards the edge of the whole optical network [41, p. 10]. Due to this reason, in this chapter, we will mainly study the application of flexible-grid technology in backbone networks.

The network can also be modelled as a three-layered architecture as shown in Figure 3.1. The application layer resides on top of the architecture including all types of services, e.g., voice, video, and data. The intermediate layer encapsulates data from the application layer with various protocols based on electronic switching and multiplexing techniques. The traffic of the electronic layer is aggregated into the optical layer, where they are carried by wavelengths. Form the viewpoint of customers, an end user's YouTube videos or business data of a company are first generated in the application layer and then passed to the electronic layer. Hundreds of such small data streams are integrated into one optical wavelength and transmitted through the network towards their destinations.

Note that it is possible for the application layer to directly access the optical layer [41, p. 7], as illustrated by optical access service in Figure 3.1. This capacity is independent of the specific protocol in the electronic layer and, thus, offers great transparency and

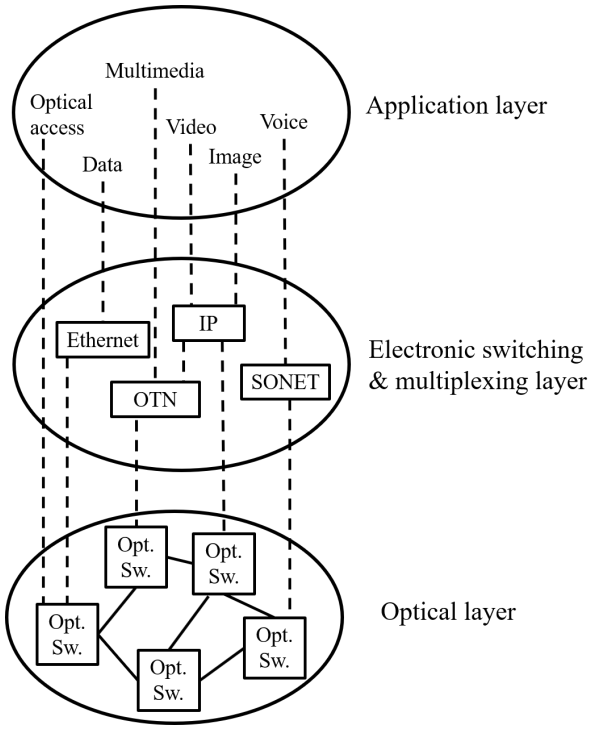

Figure 3.1: Three-layered architectural model of networks.

flexibility for large data streams. Moreover, by bypassing intermediate electronic components, the costs are also decreased significantly. This desirable feature is achieved by BV-Ts and BV-WXCs in flexible-grid optical networks, where the end users with variable data rates requests (ranging from the finest granularity to thousands of Gbps) can directly connect into the optical layer and adjust connection bandwidths according to real-time demands [29, Ch. 10].

In this chapter, we will mainly focus on resource allocation in the optical layer and consider the traffic from higher layers as determined input. This allows us to reasonably simplify the problem and achieve good network efficiency. More sophisticated cross-layer network optimization can also be carried out, but with much higher modelling complexity and computational cost.

We can also classify optical networks according to the temporal characteristics of traffic demands. In the dynamic traffic scenario, connections are added and removed in real time, and the network can adapt to the prevailing traffic patterns. However, considerable research is still required for the dynamic traffic technology to mature and find its application in real-world optical networks [42, Sec. 12]. In contrast, the static traffic scenario is still very common in current optical networks, where connections exist for months or years. Any modification of the network, including removal or addition of connections, needs to be planned periodically well in advance. As design tools aiming at long-term network planning, the resource allocation algorithms presented in this chapter mainly focus on the static traffic optical networks. The static traffic demands are given as input to the algorithms and the resource allocation problems are solved offline.

3.2 Routing and Wavelength Assignment

The routing and wavelength assignment (RWA) in the WDM networks is the most classic resource allocation problem in optical networks. The main focus of the RWA is to establish optical connections according to traffic demands. An optical connection consists of a set of fiber links connecting the source and destination nodes, and a particular wavelength for the connection [43]. The RWA thus deals with the selection of routes and wavelengths. It can be stated in terms of inputs, outputs, constraints, and objective as follows:

- *Inputs:* the network topology and set of traffic demands.
- *Outputs:* the routes and wavelengths assigned to each traffic demand.
- *Constraints:*
    1. *Wavelength continuity constraint:* the same wavelength must be assigned to all the links traversed by the connection.
    2. *Distinct wavelength constraint:* if two or more connections share a common link, each of them must be assigned a distinct wavelength.
- *Objective:* minimize the number of wavelengths used to establish all the traffic demands.

Note that we only consider modulation formats and baud rates that have suitable TRs for all the traffic demands and, thus, the QoT requirement is implicitly satisfied.

3.2.1 ILP Formulation

The network topology is denoted as (V, E), where V is the set of nodes and E is the set of links. Each link has two fibers with opposite directions and multiple spans. The set of directional links going out from node n is denoted as E_n^+, and the set of directional links coming into node n is denoted as E_n^-. The set of wavelengths on the fiber links is denoted as W.

The set of traffic demands in the RWA problem is denoted as T. We use $\texttt{src}(t)$, $\texttt{dst}(t)$, and $\texttt{wv}(t)$ to denote the source, destination, and requested number of wavelengths of the traffic demand $t \in T$, respectively[1]. Here $\texttt{src}(t), \texttt{dst}(t) \in V$ are nodes in the network, and $\texttt{wv}(t) \in \mathbb{Z}_+$ is a positive integer. The set of traffic demands T is assumed to be static and deterministic. This is because the design of backbone networks is accomplished by forecasting a certain set of traffic demands periodically in the order of several months or years [44, p. 598]. During this period, the traffic prediction is reasonably accurate and the variation of actual traffic demands is relatively slow. These variations can be handled by reconfigurable optical add-drop multiplexers installed in the network.

According to the constraints and objective of the RWA, we can obtain an integer linear programming (ILP) formulation to solve the problem optimally [45]. In this ILP formulation, the decision variables are listed below.

- $c_t^{lw} \in \mathbb{B}$: equals 1 if traffic demand $t \in T$ from node $\texttt{src}(t)$ to $\texttt{dst}(t)$ is established using wavelength w on link l, and 0 otherwise.
- $u^w \in \mathbb{B}$: equals 1 if wavelength w is used anywhere in the network, and 0 otherwise.
- $\omega_{\text{total}} \in \mathbb{Z}_+$: the maximum wavelength index used in the network.

The ILP formulation of the RWA problem can be expressed as [45]

$$\text{minimize} \quad \omega_{\text{total}} \tag{3.1}$$

$$\text{subject to} \quad \sum_{l \in E_n^-} \sum_{w \in W} c_t^{lw} = 0, \qquad \forall t \in T, n = \texttt{src}(t), \tag{3.2}$$

$$\sum_{l \in E_n^+} \sum_{w \in W} c_t^{lw} = \texttt{wv}(t), \qquad \forall t \in T, n = \texttt{src}(t), \tag{3.3}$$

$$\sum_{l \in E_n^-} \sum_{w \in W} c_t^{lw} = \texttt{wv}(t), \qquad \forall t \in T, n = \texttt{dst}(t), \tag{3.4}$$

$$\sum_{l \in E_n^+} \sum_{w \in W} c_t^{lw} = 0, \qquad \forall t \in T, n = \texttt{dst}(t), \tag{3.5}$$

[1] Here we assume that the finest granularity in the spectrum domain is defined by one wavelength. And the same modulation format, baud rate, and bandwidth are used for all the connections.

$$\sum_{l \in E_n^+} c_t^{lw} - \sum_{l \in E_n^-} c_t^{lw} = 0, \qquad \begin{array}{l} \forall t \in T, w \in W, \\ n \in V, n \neq \mathtt{src}(t), \mathtt{dst}(t), \end{array} \tag{3.6}$$

$$\sum_{t \in T} c_t^{lw} \leq 1, \qquad \forall l \in E, \forall w \in W, \tag{3.7}$$

$$\sum_{t \in T} \sum_{l \in E} c_t^{lw} \leq u^w |V|(|V|-1)|E|, \qquad \forall w \in W, \tag{3.8}$$

$$\omega_{\text{total}} \geq w u^w, \qquad \forall w \in W. \tag{3.9}$$

Equations (3.2)–(3.6) are the multicommodity flow constraint at node n. Specifically, for a traffic demand t, (3.2) and (3.3) state that the number of wavelengths going into its source node is 0, whereas the number of outgoing wavelengths equals $\mathtt{wv}(t)$. Similarly, (3.4) and (3.5) state that at the destination node of t, the incoming number of wavelengths equals $\mathtt{wv}(t)$ and outgoing number of wavelengths is 0. In (3.6), if node n is an intermediate node on the path of t, the traffic into the node should equals the traffic out, since no traffic is added or dropped at node n. Constraints (3.2)–(3.6) ensure that all the traffic demands are satisfied. In addition, by imposing no adding or dropping flows at intermediate nodes, the wavelength continuity constraint is implicitly guaranteed as the same wavelength is used on all the links along the path. Inequality (3.7) represents the distinct wavelength constraint such that no two connections share the same wavelength on one link. Expression (3.8) ensures $u^w = 1$ when wavelength w is used on any link by any connection. Expression (3.9) calculates the highest wavelength index used in the network.

The complexity of the ILP formulation (3.1)–(3.9) is related to the number of binary variables and constraints. The number of variables c_t^{lw} is equal to $|T||E||W|$, where $|T|$ is the number of traffic demands, $|E|$ is the number of links in the network, and $|W|$ is the number of wavelengths in one link. There are also $|W|$ variables u^w and one variable ω_{total}. Hence, the total number of variables is $O(|T||E||W|)$. For the number of constraints, (3.2)–(3.5) have $4|T|$ constraints, (3.6) has approximately $|T||W||V|$ constraints, and (3.7) corresponds to $|E||W|$ constraints. Each of (3.8) and (3.9) consists of $|W|$ constraints. As a result, the number of constraints is $O(|T||W||V| + |E||W|)$, which is dominated by the flow conservation constraint (3.6).

The ILP formulation in (3.1)–(3.9) searches all possible combinations of links to form paths for every connection and, thus, is referred to as link-based formulation. The optimal solution is guaranteed in the link-based formulation. On the other hand, the RWA is known to be an NP-hard problem [46]. Therefore, it is not possible to obtain the optimal solution of the ILP formulation (3.1)–(3.9) for realistic optical networks within reasonable time. Fortunately, the RWA problem can be simplified by decoupling the problem into two separate subproblems: the routing subproblem and the wavelength assignment subproblem. By decomposing the original RWA problem, a reasonable computational complexity can be achieved at the cost of suboptimal solutions.

3.2.2 Routing Subproblem

The routing subproblem can be stated as follows:

- *Inputs:* the network topology and set of traffic demands.
- *Output:* the route assigned to each traffic demand.
- *Constraint:* every traffic demand is provisioned.
- *Objective:* minimize the maximum number of paths used by any single links.

For the sake of simplicity, we assume that if multiple wavelengths are requested by one traffic demand, all these wavelengths are assigned to the same route. In the routing subproblem, the wavelength assignment is neglected. This is equivalent to having wavelength converters with unlimited capability at every node in the network. Unlike the link-based formulation in Section 3.2.1 where every possible combination of links are searched, here we select route for every connection from a set of precalculated candidates. This kind of formulation is hence referred to as path-based formulation. According to the problem statement, we can formulate a low complexity ILP to solve the routing subproblem. Let us first define parameters used in the routing ILP formulation.

- $k \in \mathbb{Z}_+$: The number of candidate paths precalculated for every pair of nodes before formulating the routing ILP. Usually $k = 12$ [47] is sufficient to obtain close-to-optimal paths.
- P_t: the set of k candidate paths for traffic demand $t \in T$, which can be obtained using the k-shortest path algorithm [48].
- P_t^l: the set of candidate paths in P_t using a particular link $l \in E$.

The variables involved in the ILP formulation are

- $x_t^p \in \mathbb{B}$: equals 1 if a candidate path $p \in P_t$ is selected, and 0 otherwise.
- $y_l \in \mathbb{Z}_+$: the number of paths using link l.
- $Y \in \mathbb{Z}_+$: maximum number of paths among all the links.

The routing ILP formulation can be expressed as [49]

$$\underset{x_t^p, y_l, Y}{\text{minimize}} \quad Y \tag{3.10}$$

$$\text{subject to} \quad \sum_{p \in P_t} x_t^p = 1, \qquad \forall t \in T, \tag{3.11}$$

$$y_l = \sum_{t \in T} \sum_{p \in P_t^l} x_t^p, \qquad \forall l \in E, \tag{3.12}$$

$$Y \geq y_l, \qquad \forall l \in E. \tag{3.13}$$

Constraint (3.11) ensures that the required number of wavelength of traffic demand $t \in T$ is satisfied. Note that (3.11) assumes that if multiple wavelengths are requested by one traffic demand, all these wavelengths are assigned to the same route. Equation (3.12) calculates the number of paths passing through link l, and inequality (3.13) defines the

maximum number of paths among all the links as $Y \geq \max_{l \in E} y_l$. The final output is one route p_t selected for all $t \in T$.

The number of variables x_t^p is $k|T|$, the number of variables y_l is $|E|$, and there is one variable Y. As a result, the number of variables in the routing ILP formulation is $O(k|T|)$. The number of constraints (3.11) is $|T|$, the number of constraints (3.12) is $|E|$, and there are $|E|$ inequalities (3.13). Hence the number of constraints is $O(|T|)$. Obviously, the routing ILP formulation is much simpler than the original RWA ILP formulation (3.1)–(3.9).

3.2.3 Wavelength Assignment Subproblem

After obtaining the routes for all the traffic demands, we can formulate another ILP to solve the wavelength assignment subproblem, which can be stated as follows:

- *Inputs:* the network topology, set of traffic demands, and selected route for each traffic demand.
- *Output:* the wavelengths assigned to all the traffic demands.
- *Constraints:*
  1. Wavelength continuity constraint
  2. Distinct wavelength constraint
- *Objective:* minimize the number of wavelengths used to establish all the traffic demands.

One additional parameter is used in the wavelength assignment ILP formulation

- T^l: the set of traffic demands whose routes use link l, i.e., $T^l = \{t \mid l \in p_t, t \in T\}$, where $l \in p_t$ means that route p_t uses link l.

The variables in the ILP formulation are

- $\omega_{\text{total}} \in \mathbb{Z}_+$: the highest wavelength index used by any connection in the network.
- $x_{t,i}^w \in \mathbb{B}$: equals 1 if the i-th wavelength request of traffic demand t uses wavelength $w \in W$, and 0 otherwise, where $i \in \{1, \ldots, \mathtt{wv}(t)\}$.

The wavelength assignment ILP can be formulated as [50]

$$\underset{x_{t,i}^w, \omega_{\text{total}}}{\text{minimize}} \quad \omega_{\text{total}} \tag{3.14}$$

$$\text{subject to} \quad \sum_w x_{t,i}^w = 1, \qquad \forall t \in T, i \in \{1, \ldots, \mathtt{wv}(t)\}, \tag{3.15}$$

$$\sum_{t \in T^l} \sum_{i=1}^{\mathtt{wv}(t)} x_{t,i}^w \leq 1, \qquad \forall l \in E, \forall w \in W. \tag{3.16}$$

Expression (3.15) ensures that the requested wavelengths of all the traffic demands are satisfied. It also implicitly imposes the wavelength continuity constraint. Inequality (3.16) guarantees that multiple traffic demands sharing one common link must use different wavelengths, i.e., the distinct wavelength constraint.

Suppose the maximum number of requested wavelengths by one traffic demand is U. The number of variables in the ILP formulation is $O(U|T||W|)$. The number of constraints (3.15) is $O(U|T|)$, and the number of constraints (3.16) is $|E||W|$, so the total number of constraints is $O(|E||W|+U|T|)$. Compared with the original ILP formulation of the RWA problem, which has $O(|T||E||W|)$ variables and $O(|T||V| + |E||W|)$ constraints, the wavelength assignment ILP formulation is simpler if U is well below both $|E|$ and $|V|$.

3.3 Routing and Spectrum Assignment

RSA is used to find the appropriate route and suitable spectrum for a traffic demand in flexible-grid optical networks. It is equivalent to the RWA problem in fixed-grid WDM networks [51]. On the other hand, the RSA problem is much more complicated than its WDM counterpart due to the variable modulation format and fine-granular bandwidth (down to 3.125 GHz) offered by flexible-grid optical networks [3]. As a result, a traffic demand with a large data rate request would require multiple contiguous spectrum slots for transmission, which is the so-called spectrum contiguity constraint [51]. Its purpose is to reduce the number of transponders used in the network.

Assuming that all the traffic demands use the same modulation format, the RSA problem can be stated as

- *Inputs:* the network topology and set of traffic demands.
- *Outputs:* the routes and spectrum slots assigned to all the traffic demands.
- *Constraints:*
    1. *Spectrum continuity constraint:* the same spectrum slots must be assigned to all the links traversed by a connection.
    2. *Spectrum contiguity constraint:* contiguous spectrum slots should be assigned to one path.
    3. *Nonoverlapping spectrum constraint:* if two or more connections share a common link, their spectrum slots should be distinct and nonoverlapping.
- *Objective:* minimize the number of spectrum slots used to establish all the traffic demands.

3.3.1 ILP Formulation

Similar to the notation of the RWA problem in Section 3.2, we use (V, E) to denote the network, where V is the set of nodes and E is the set of links. Each link consists of two fibers with opposite directions and multiple spans. The ordered set of spectrum slots on

each fiber link is denoted as $S = \{s_1, s_2, \ldots, s_{|S|}\}$. The set of static traffic demands is denoted as T. For each traffic demand $t \in T$, we use $\texttt{src}(t), \texttt{dst}(t), \texttt{spc}(t)$ to denote the source, destination, and number of spectrum slots including guardbands requested by t, respectively.

To simplify the formulation, it is assumed that for each traffic demand t a set of k distinct routes $P_t = \{p_{t,1}, p_{t,2}, \ldots, p_{t,k}\}$ is computed beforehand, out of which one route is chosen for the demand. Each route $p_{t,i} \in P_t$ for $i \in \{1, 2, \ldots, k\}$ is an ordered set of links so that nodes $\texttt{src}(t)$ and $\texttt{dst}(t)$ are connected. Therefore, if link l satisfies $l \in p_{t_1,i} \cap p_{t_2,j}$, it means that both routes $p_{t_1,i}$ and $p_{t_2,j}$ use link l for $l \in E$. Furthermore, with a slight abuse of notation, we use $P_{t_1} \cap P_{t_2} \neq \varnothing$ to denote the situation that there exist routes $p_{t_1,i} \in P_{t_1}$ and $p_{t_2,j} \in P_{t_2}$ such that $p_{t_1,i} \cap p_{t_2,j} \neq \varnothing$.

The decision variables in the ILP formulation are

- $f_t \in \mathbb{Z}_+$: the starting spectrum slot index of traffic demand $t \in T$.
- $\delta_{t_1,t_2} \in \mathbb{B}$: equals 1 if the starting spectrum slot[2] index of demand t_1 is smaller than that of t_2, i.e., $f_{t_1} < f_{t_2}$, and 0 otherwise.
- $y_{t,i} \in \mathbb{B}$: equals 1 if traffic demand t uses route $p_{t,i}$, and 0 otherwise, $t \in T$ and $p_{t,i} \in P_t$.
- $\omega_{\text{total}} \in \mathbb{Z}_+$: the maximum spectrum slot index used in the network.

The ILP formulation of the RSA problem can be expressed as [51]

$$\text{minimize} \quad \omega_{\text{total}} \tag{3.17}$$

$$\text{subject to} \quad f_t + \texttt{spc}(t) \leq |S|, \qquad \forall t \in T, \tag{3.18}$$

$$\delta_{t_1,t_2} + \delta_{t_2,t_1} = 1, \qquad \forall t_1, t_2 \in T : P_{t_1} \cap P_{t_2} \neq \varnothing, \tag{3.19}$$

$$f_{t_2} - f_{t_1} < |S| \cdot \delta_{t_1,t_2}, \qquad \forall t_1, t_2 \in T : P_{t_1} \cap P_{t_2} \neq \varnothing, \tag{3.20}$$

$$f_{t_1} - f_{t_2} < |S| \cdot \delta_{t_2,t_1}, \qquad \forall t_1, t_2 \in T : P_{t_1} \cap P_{t_2} \neq \varnothing, \tag{3.21}$$

$$f_{t_1} + \texttt{spc}(t_1) \cdot y_{t_1,i} - f_{t_2} < |S| \cdot (3 - \delta_{t_1,t_2} - y_{t_1,i} - y_{t_2,j}), \quad \forall t_1, t_2 \in T, \; p_{t_1,i} \in P_{t_1}, p_{t_2,j} \in P_{t_2} : \; p_{t_1,i} \cap p_{t_2,j} \neq \varnothing, \tag{3.22}$$

$$f_{t_2} + \texttt{spc}(t_2) \cdot y_{t_2,j} - f_{t_1} < |S| \cdot (3 - \delta_{t_2,t_1} - y_{t_1,i} - y_{t_2,j}), \quad \forall t_1, t_2 \in T, \; p_{t_1,i} \in P_{t_1}, p_{t_2,j} \in P_{t_2} : \; p_{t_1,i} \cap p_{t_2,j} \neq \varnothing, \tag{3.23}$$

$$\sum_{p_{t,i} \in P_t} y_{t,i} = 1, \qquad \forall t \in T, \tag{3.24}$$

$$\omega_{\text{total}} \geq f_t, \qquad \forall t \in T. \tag{3.25}$$

The objective of the RSA formulation (3.17)–(3.25) is to minimize the maximum spectrum slot index used in the network, which is computed by constraint (3.25). Constraint (3.18) guarantees that the starting slot of each traffic demand leaves enough room

[2]The starting spectrum slot of a connection is defined as its smallest spectrum slot.

for its requested number of spectrum slots. Constraints (3.19)–(3.21) manage starting slot ordering for all traffic demand pairs that potentially share some fiber link. They compute if the starting slot of one traffic demand in the pair is lower than that of the other one. Inequalities (3.22)–(3.23) impose the spectrum nonoverlapping constraint. Constraint (3.24) imposes that one route is selected for each traffic demands.

Let us now turn our attention to the scalability of the ILP formulation (3.17)–(3.25). The number of the f_t variables equals $|T|$. The number of the δ_{t_1,t_2} variables is at most $|T|(|T|-1)$ when every pair of traffic demands has some shared fiber link. The number of the $y_{t,i}$ variables is $k|T|$. So the total number of variables is $O(|T|^2)$. In terms of the number of constraints, expression (3.18) has $|T|$ constraints. Expressions (3.19)–(3.21) have at most $3|T|(|T|-1)$ constraints. Expressions (3.22)–(3.23) have at most $2k^2|T|(|T|-1)$ constraints. Expression (3.25) has $|T|$ constraints. The total number of constraints is $O(k^2|T|^2)$.

The computational complexity of the exact ILP formulation (3.17)–(3.25) is very high. For large size networks, we have to resort to heuristics. The original RSA is decomposed into two subproblems: the routing subproblem and the spectrum assignment subproblem. Similar to the RWA, these two subproblems can be formulated as ILPs. However, due to the large number of spectrum slots in flexible-grid optical networks and the spectrum contiguity constraint, the ILPs of the subproblems can still have relatively high complexity. Alternatively, the RSA problem can also be solved by greedy algorithms, which offer good quality solutions with much lower computational complexity.

3.3.2 Heuristic Algorithm for RSA

One simple yet effective method is to serve the traffic demands sequentially in a particular order, which is referred to as the connection list (CL) method [49, 52]. Each time a new traffic demand is served, we first calculate the k-shortest candidate paths[3] for that demand. Since there are already-served traffic demands existing in the network, the minimum allowable start spectrum slots of the candidate paths are different. We select the path that minimizes the index of the maximum spectrum slots used in the whole network to serve the current traffic demand, and then move on to process the next one. This algorithm searches for the locally optimal RSA solution that minimizes the estimated spectrum usage for the current traffic demand.

There are many methods to choose the order of traffic demands. For example, we can order the traffic demands according to their requested data rates, and serve first the demand with the highest data rate. Alternatively, we can order the traffic demands according to the distance from their sources to destinations. Metaheuristics such as simulated annealing can also be applied to optimize the ordering of traffic demands [50] at the cost of higher computational complexity.

[3]Usually $k = 12$ is sufficient to yield good solutions.

3.4 TR-Model-Based RMSA

In the previous section, the same modulation format is applied to all the optical connections. In flexible-grid optical networks, however, the transponders are enabled to adapt bit rate and bandwidth for a given traffic demand. This is realized by adjusting the transmission parameters such as modulation formats or coding rate of optical connections according to the requirements of and resources allocated to individual traffic demands. Actually, the spectrum allocated to one optical connection can affect other connections in the network by changing their QoTs and available network resources. Therefore, similar to the RWA and RSA problems in previous sections, the allocation of modulation format should be planned over the network globally to optimize the network performance and resource utilization.

To include the modulation format allocation, the RSA problem is extended to the routing, modulation format, and spectrum allocation (RMSA) problem [49]. In addition to the original constraints in the RSA problem, the RMSA has a new constraint on the feasibility of modulation formats based on the TR model:

- *TR constraint:* the TR of a modulation format used over a path should be no less than the length of the path.

The problem statement of the RMSA is very similar to the RSA problem

- *Inputs:* the network topology, set of traffic demands, and set of available modulation formats.
- *Outputs:* the routes, modulation formats, and spectrum slots assigned to all the traffic demands.
- *Constraints:*
  1. Spectrum continuity constraint
  2. Spectrum contiguity constraint
  3. Nonoverlapping spectrum constraint
  4. TR constraint
- *Objective:* minimize the number of spectrum slots used to establish all the traffic demands.

Let us present an ILP formulation of the RMSA problem based on precalculated routes [49]. The notation of the RMSA problem follow those of the RSA problem, except that the required number of spectrum slots $\texttt{spc}(t)$ is replaced by the required data rate $\texttt{dtr}(t)$ for traffic demand $t \in T$. Additionally, we use $M = \{c_1, c_2, \ldots, c_R\}$ to denote the ascendingly ordered set of R available modulation formats, where c_j is the SE of the j-th modulation format for $j \in \{1, 2, \ldots, R\}$. Each precalculated route $p_{t,i} \in P_t$ is associated with a subset $M(p_{t,i}) \subseteq M$, whose elements are feasible over the path according to the TR model. Among the modulation formats in $M(p_{t,i})$, $c(p_{t,i}) = \max\{c \mid c \in M(p_{t,i})\}$ is

used to denote the one with the highest SE, which is always used for $p_{t,i}$. The number of spectrum slots of t over route $p_{t,i}$ is hence

$$b_{t,i} = \lceil \mathtt{dtr}(t)/c(p_{t,i}) \rceil + B, \tag{3.26}$$

where B is the number of spectrum slots used by the guardband. Note that under the assumption of a transparent optical network, all the traffic demands can be transmitted successfully without regeneration and, thus, we have $\cup_{p_{t,i} \in P_t} M(p_{t,i}) \neq \varnothing$ for all $t \in T$.

The ILP formulation of the RSMA can be expressed as [49]

$$\text{minimize} \quad \omega_{\text{total}} \tag{3.27}$$

$$\text{subject to} \quad f_t + \sum_{p_{t,i} \in P_t} b_{t,i} \cdot y_{t,i} \leq |S|, \qquad \forall t \in T, \tag{3.28}$$

$$\delta_{t_1,t_2} + \delta_{t_2,t_1} = 1, \qquad \forall t_1, t_2 \in T : P_{t_1} \cap P_{t_2} \neq \varnothing, \tag{3.29}$$

$$f_{t_2} - f_{t_1} < |S| \cdot \delta_{t_1,t_2}, \qquad \forall t_1, t_2 \in T : P_{t_1} \cap P_{t_2} \neq \varnothing, \tag{3.30}$$

$$f_{t_1} - f_{t_2} < |S| \cdot \delta_{t_2,t_1}, \qquad \forall t_1, t_2 \in T : P_{t_1} \cap P_{t_2} \neq \varnothing, \tag{3.31}$$

$$f_{t_1} + b_{t_1,i} \cdot y_{t_1,i} - f_{t_2} < |S| \cdot (3 - \delta_{t_1,t_2} - y_{t_1,i} - y_{t_2,j}), \quad \begin{array}{l} \forall t_1, t_2 \in T, \\ p_{t_1,i} \in P_{t_1}, p_{t_2,j} \in P_{t_2} : \\ p_{t_1,i} \cap p_{t_2,j} \neq \varnothing, \end{array} \tag{3.32}$$

$$f_{t_2} + b_{t_2,j} \cdot y_{t_2,j} - f_{t_1} < |S| \cdot (3 - \delta_{t_2,t_1} - y_{t_1,i} - y_{t_2,j}), \quad \begin{array}{l} \forall t_1, t_2 \in T, \\ p_{t_1,i} \in P_{t_1}, p_{t_2,j} \in P_{t_2} : \\ p_{t_1,i} \cap p_{t_2,j} \neq \varnothing, \end{array} \tag{3.33}$$

$$\sum_{p_{t,i} \in P_t} y_{t,i} = 1, \qquad \forall t \in T, \tag{3.34}$$

$$\omega_{\text{total}} \geq f_t, \qquad \forall t \in T. \tag{3.35}$$

Note that the required number of spectrum slots $\mathtt{spc}(t)$ for traffic demand t in the ILP formulation of the RSA problem is replaced by the connection bandwidth $b_{t,i}$ on the precalculated route $p_{t,i}$. Besides this difference, the ILP formulations of the RSA and RSMA problems are the same. Consequently, the heuristic algorithm in Section 3.3.2 that allocates the traffic demands sequentially according to a certain ordering can also be used here [49].

3.5 GN-Model-Based RMSA

In Sections 3.2 and 3.3, the QoTs in the RWA and RSA problems are implicitly assumed to be satisfactory for all the demands. In Section 3.4, the TR model is used to guarantee the QoTs in the RMSA problem. However, to fully exploit the advantages offered by flexible-grid optical networks, it is necessary to incorporate the GN model into the RMSA problem to achieve more accurate QoT estimation.

The GN model based RMSA (GN-RMSA) problem in flexible-grid optical networks is stated as

- *Inputs:* the network topology, set of traffic demands, and set of available modulation formats.
- *Outputs:* the routes, modulation formats, and spectrum slots assigned to all the traffic demands.
- *Constraints:*
  1. Spectrum continuity constraint
  2. Spectrum contiguity constraint
  3. Nonoverlapping spectrum constraint
  4. QoT constraint based on the GN model
- *Objective:* minimize the number of spectrum slots used to establish all the traffic demands.

Here, the QoT constraint requires that all the traffic demands should have satisfactory QoTs, which are calculated based on the GN model and SNR thresholds of the allocated modulation formats in Sections 2.6 and 2.7.

3.5.1 ILP Formulation

Note that in the GN model, the NLI PSD in (2.17) contains nonlinear functions. If the QoT constraint (2.19) is included directly into the GN-RMSA problem, the resulting optimization will be a mixed integer nonlinear programming (MINLP) problem [Paper A and B]. This would increase the computational complexity significantly and impact the scalability of the algorithm negatively. To solve this problem, lookup tables of the nonlinear functions in the GN model are constructed to facilitate the computation of NLIs [52], based on which a link-based mixed integer linear programming (MILP) formulation is proposed for the GN-RMSA problem. Here we will introduce the MILP formulation [52]. To simplify the original formulation and keep the notation consistent with that in Sections 3.3 and 3.4, we rewrite the original MILP [52] as a path-based formulation.

The MILP of the GN-RMSA problem involves many input parameters and decision variables. For completeness and clarity of the problem formulation, the definitions of all the symbols and notation are summarized below regardless of any possible repetitions. The input parameters in the MILP formulation of the GN-RMSA problem are

- (V, E): the topology of the network, where V and E denote the sets of nodes and links.
- $N_l \in \mathbb{Z}_+$: the number of spans on link $l \in E$.
- $S = \{s_1, s_2, \ldots, s_{|S|}\}$: the ordered set of spectrum slots on each fiber link, where $|S|$ is the total number of available spectrum slots per link.

- T: the set of static traffic demands, where each traffic demand $t \in T$ consists of a triplet $(\texttt{src}(t), \texttt{dst}(t), \texttt{dtr}(t))$ denoting the source, destination, and required data rate of t.
- T^2: the set of all the traffic demand pairs, i.e., $T^2 = \{(t_1, t_2) \mid t_1, t_2 \in T, t_1 \neq t_2\}$.
- $P_t = \{p_{t,1}, p_{t,2}, \ldots, p_{t,k}\}$: The set of k precalculated routes for traffic demand $t \in T$, where each precalculated route $p_{t,i} \in P_t$ is an ordered set of links connecting $\texttt{src}(t)$ and $\texttt{dst}(t)$. We write $l \in p_{t_1,i} \cap p_{t_2,j}$ if two candidate routes $p_{t_1,i}$ and $p_{t_2,j}$ share a link $l \in E$, and use $P_{t_1} \cap P_{t_2} \neq \varnothing$ to denote the situation where there exist routes $p_{t_1,i} \in P_{t_1}$ and $p_{t_2,j} \in P_{t_2}$ such that $p_{t_1,i} \cap p_{t_2,j} \neq \varnothing$.
- $b_{t,c} = \lceil \texttt{dtr}(t)/c \rceil + B \in \mathbb{Z}_+$: the number of spectrum slots required by traffic demand $t \in T$ using modulation format $c \in M$, where B is the number of spectrum slots used by the guardband.
- $K = \{1, \ldots, k\}$: the set of indices for precalculated routes in $P_t, \forall t \in T$.
- $M = \{c_1, c_2, \ldots, c_{|M|}\}$: the ascendingly ordered set of available modulation formats, where $c_j \in M$ is the SE of the j-th available modulation format.
- $H = \{0, 1, \ldots, 2|S|\}$: the set of integers from 0 to $2|S|$.
- $\mathrm{SNR}_c^{\mathrm{th}} \in \mathbb{R}_+$: the SNR threshold of modulation format $c \in M$.
- $J_{t,c,h}^{\mathrm{XCI}} = \mu \ln\left((h + b_{t,c})/(h - b_{t,c})\right) \in \mathbb{R}_+$: The XCI PSD introduced by traffic demand $t \in T$ to another traffic demand when t is assigned modulation format $c \in M$ and their center frequency spacing is $h \in H$ in the number of half spectrum slots. Here $\mu = 3\gamma^2/(2\pi\alpha|\beta_2|)$ and α, β_2, and γ are parameters related to the physical property of optical fibers defined in Section 2.6.
- $J_{t,c}^{\mathrm{SCI}} = \mu \ln\left(\rho(\mathrm{BW} \cdot b_{t,c})^2\right) \in \mathbb{R}_+$: the SCI PSD for traffic demand $t \in T$ when it is assigned modulation format $c \in M$, where BW is the bandwidth of one spectrum slot and $\rho = \pi^2|\beta_2|/(2\alpha)$.
- $G \in \mathbb{R}_+$: the uniform PSD for all the traffic demands.
- $G^{\mathrm{ASE}} \in \mathbb{R}_+$: the ASE PSD per span.
- $\theta \in \mathbb{R}_+$: a big enough real number.

Here the values of $J_{t,c,h}^{\mathrm{XCI}}$ and $J_{t,c}^{\mathrm{SCI}}$ are precalculated and stored in lookup tables, which will be accessed by indicator variables in the MILP formulation to perform the nonlinear computations in the GN model. The decision variables in the MILP formulation of the GN-RMSA problem are

- $f_t \in \mathbb{Z}_+$: the starting spectrum slot index of traffic demand $t \in T$.
- $\delta_{t_1,t_2} \in \mathbb{B}$: equals 1 if the starting spectrum slot index of traffic demand t_1 is smaller than that of t_2, i.e., $f_{t_1} < f_{t_2}$, and 0 otherwise, $(t_1, t_2) \in T^2$.

- $y_{t,i} \in \mathbb{B}$: equals 1 if traffic demand t uses route $p_{t,i}$, and 0 otherwise, $t \in T$ and $p_{t,i} \in P_t$.
- $u_{t_1,t_2} \in \mathbb{B}$: equals 1 if traffic demands t_1 and t_2 share some common link, and 0 otherwise, $(t_1, t_2) \in T^2$.
- $\omega_{\text{total}} \in \mathbb{Z}_+$: the maximum spectrum slot index used in the network.
- $\texttt{spc}(t) \in \mathbb{Z}_+$: the number of spectrum slots allocated to traffic demand $t \in T$.
- $z_{t,i} \in \mathbb{Z}$: equals the number of spectrum slots used on the candidate route $p_{t,i} \in P_t$, if $p_{t,i}$ is selected by traffic demand $t \in T$, and 0 otherwise.
- $m_{t,c} \in \mathbb{B}$: equals 1 if traffic demand t uses modulation format c, and 0 otherwise, $t \in T$ and $c \in M$.
- $\Delta_{t_1,t_2,h,c} \in \mathbb{B}$: equals 1 if the center frequency spacing between traffic demands t_1 and t_2 is h in the number of half spectrum slots and $m_{t_2,c} = 1$, and 0 otherwise, $h \in H$ and $(t_1, t_2) \in T^2$.
- $F^{\text{abs}}_{t_1,t_2} \in \mathbb{R}_+$: an auxiliary variable that equals the absolute value of center frequency spacing between traffic demands t_1 and t_2 in the number of half spectrum slots.
- $\kappa_{t_1,t_2,l} \in \mathbb{B}$: equals 1 if traffic demands t_1 and t_2 share link l, and 0 otherwise, $(t_1, t_2) \in T^2, l \in E$.
- $\sigma_{t,l} \in \mathbb{B}$: equals 1 if traffic demand t uses link l, and 0 otherwise, $t \in T, l \in E$.
- $n^{\text{XCI}}_{t_1,t_2,l} \in \mathbb{R}_+$: the upper bound of the XCI PSD generated from traffic demands t_2 to t_1 on link l, $(t_1, t_2) \in T^2, l \in E$.
- $n^{\text{NLI}}_{t,l} \in \mathbb{R}_+$: the upper bound of the NLI PSD for traffic demand t on link l, $t \in T, l \in E$.

The MILP formulation of the GN-RMSA problem is originally presented in [52]. Here we rewrite the formulation with clearer constraint expressions and explanation of its linearity.

$$\text{minimize} \quad \omega_{\text{total}} \tag{3.36}$$

$$\text{subject to} \quad \sum_{i \in K} y_{t,i} = 1, \qquad \forall t \in T, \tag{3.37}$$

$$z_{t,i} = y_{t,i} \cdot \sum_{c \in M} b_{t,c} m_{t,c}, \qquad \forall t \in T, i \in K, \tag{3.38}$$

$$\texttt{spc}(t) = \sum_{i \in K} z_{t,i}, \qquad \forall t \in T, \tag{3.39}$$

$$\sigma_{t,l} = \sum_{i : l \in p_{t,i}} y_{t,i}, \qquad \forall t \in T, l \in E, \tag{3.40}$$

$$\kappa_{t_1,t_2,l} = \sigma_{t_1,l} \cdot \sigma_{t_2,l}, \qquad \forall (t_1, t_2) \in T^2, l \in E, \tag{3.41}$$

$$u_{t_1,t_2} = \sum_{l \in E} \kappa_{t_1,t_2,l}, \qquad \forall (t_1,t_2) \in T^2, \tag{3.42}$$

$$f_t + \mathtt{spc}(t) \leq |S|, \qquad \forall t \in T, \tag{3.43}$$

$$\delta_{t_1,t_2} + \delta_{t_2,t_1} = 1, \qquad \forall (t_1,t_2) \in T^2 : P_{t_1} \cap P_{t_2} \neq \varnothing, \tag{3.44}$$

$$F^{\text{abs}}_{t_1,t_2} = \left| 2f_{t_2} + \mathtt{spc}(t_2) - 2f_{t_1} - \mathtt{spc}(t_1) \right|, \qquad \forall (t_1,t_2) \in T^2, \tag{3.45}$$

$$\sum_{c \in M} m_{t,c} = 1, \qquad \forall t \in T, \tag{3.46}$$

$$\sum_{h \in H} \Delta_{t_1,t_2,h,c} = m_{t_2,c}, \qquad \forall (t_1,t_2) \in T^2, c \in M, \tag{3.47}$$

$$\sum_{h \in H, c \in M} h\Delta_{t_1,t_2,h,c} = u_{t_1,t_2} \cdot F^{\text{abs}}_{t_1,t_2}, \qquad \forall (t_1,t_2) \in T^2, \tag{3.48}$$

$$n^{\text{XCI}}_{t_1,t_2,l} = \kappa_{t_1,t_2,l} \cdot \sum_{h \in H, c \in M} \Delta_{t_1,t_2,h,c} J^{\text{XCI}}_{t_2,c,h}, \qquad \forall (t_1,t_2) \in T^2, l \in E, \tag{3.49}$$

$$n^{\text{NLI}}_{t_2,l} = \sigma_{t_2,l} \cdot \sum_{c \in M} m_{t_2,c} J^{\text{SCI}}_{t_2,c} + \sigma_{t_2,l} \cdot \sum_{t_1:(t_1,t_2) \in T^2} n^{\text{XCI}}_{t_1,t_2,l}, \qquad \forall t_2 \in T, l \in E, \tag{3.50}$$

$$\sum_{i \in K} p_{t,i} \sum_{l \in p_{t,i}} N_l (G^{\text{ASE}} + n^{\text{NLI}}_{t,l}) \leq G \sum_{c \in M} m_{t,c} / \text{SNR}^{\text{th}}_c, \qquad \forall t \in T, \tag{3.51}$$

$$\omega_{\text{total}} \geq f_t + \mathtt{spc}(t), \qquad \forall t \in T. \tag{3.52}$$

To simplify the MILP formulation (3.36)–(3.52), some of the constraints are not written in their linear forms. Now let us elaborate on the meaning of all the constraints and show their equivalence to linear expressions. Constraint (3.37) ensures that one candidate route is selected for each traffic demand. Constraint (3.38) is a product of the binary variable $y_{t,i}$ and integer $\sum_{c \in M} b_{t,c} m_{t,c}$. Specifically, $z_{t,i} = \sum_{c \in M} b_{t,c} m_{t,c}$ if the candidate route $i \in K$ and modulation c are selected by t and 0 otherwise. It is equivalent to the following linear constraints for $t \in T, i \in K$

$$\begin{aligned} z_{t,i} &\leq |S| \cdot y_{t,i}, \\ z_{t,i} &\leq \sum_{c \in M} b_{t,c} m_{t,c}, \\ z_{t,i} &\geq \sum_{c \in M} b_{t,c} m_{t,c} + |S| \cdot (y_{t,i} - 1), \\ z_{t,i} &\geq 0. \end{aligned} \tag{3.53}$$

Constraint (3.39) calculates the number of spectrum slots for a traffic demand by sum-

ming over all its candidate routes. Constraint (3.40) checks if a link is used by a traffic demand. Constraint (3.41), which is a product of two binary variables, computes if one link is shared by two traffic demands. It is equivalent to

$$\begin{aligned}
&\kappa_{t_1,t_2,l} \leq \sigma_{t_1,l}, \\
&\kappa_{t_1,t_2,l} \leq \sigma_{t_2,l}, \\
&\kappa_{t_1,t_2,l} \geq \sigma_{t_1,l} + \sigma_{t_2,l} - 1,
\end{aligned} \tag{3.54}$$

for $(t_1, t_2) \in T^2, l \in E$. Constraint (3.42) determines if two traffic demands share any common link. Constraint (3.43) imposes an upper bound on the starting spectrum slot index and bandwidth of traffic demands. Constraint (3.44) specifies the order of traffic demands in the spectrum. Constraint (3.45) calculates the absolute value of the center frequency difference between two traffic demands, measured in multiples of half a spectrum slot. It is equivalent to

$$\begin{aligned}
&F_{t_1,t_2} = 2f_{t_2} + \mathtt{spc}(t_2) - 2f_{t_1} - \mathtt{spc}(t_1), \\
&F_{t_1,t_2} = F^{+}_{t_1,t_2} - F^{-}_{t_1,t_2}, \\
&F^{+}_{t_1,t_2} \geq 0, \\
&F^{+}_{t_1,t_2} \leq |S| \cdot \delta_{t_1,t_2}, \\
&F^{-}_{t_1,t_2} \geq 0, \\
&F^{-}_{t_1,t_2} \leq |S| \cdot \delta_{t_2,t_1}, \\
&F^{\mathrm{abs}}_{t_1,t_2} = F^{+}_{t_1,t_2} + F^{-}_{t_1,t_2},
\end{aligned} \tag{3.55}$$

for all $(t_1, t_2) \in T^2$, where $F_{t_1,t_2} \in \mathbb{R}$ is the center frequency spacing between traffic demands t_1 and t_2; $F^{+}_{t_1,t_2} \in \mathbb{R}_+$ is an auxiliary variable that equals F_{t_1,t_2} if $F_{t_1,t_2} > 0$, and 0 otherwise; $F^{-}_{t_1,t_2} \in \mathbb{R}_+$ is an auxiliary variable that equals $-F_{t_1,t_2}$ if $F_{t_1,t_2} < 0$, and 0 otherwise. Constraint (3.46) ensures that one modulation format is selected for each traffic demand. Equations (3.47) and (3.48) are related to the indicator variable $\Delta_{t_1,t_2,h,c}$, which is used to access the value of $J^{\mathrm{XCI}}_{t,c,h}$ stored in the lookup table. Specifically, the center frequency spacing at the right hand side of (3.48) is given by the indicator variable and the left hand side of (3.48) is calculated from the spectrum allocation. The product of the binary variable u_{t_1,t_2} and the continuous variable $F^{\mathrm{abs}}_{t_1,t_2}$ is equivalent to

$$\begin{aligned}
&\sum_{h \in H, c \in M} h\Delta_{t_1,t_2,h,c} \leq |S| \cdot u_{t_1,t_2}, \\
&\sum_{h \in H, c \in M} h\Delta_{t_1,t_2,h,c} \leq F^{\mathrm{abs}}_{t_1,t_2}, \\
&\sum_{h \in H, c \in M} h\Delta_{t_1,t_2,h,c} \geq F^{\mathrm{abs}}_{t_1,t_2} + |S| \cdot (u_{t_1,t_2} - 1), \\
&\sum_{h \in H, c \in M} h\Delta_{t_1,t_2,h,c} \geq 0,
\end{aligned} \tag{3.56}$$

for all $(t_1, t_2) \in T^2$. Constraint (3.49) calculates the XCI PSD from traffic demand t_2 to t_1. This is realized by first checking if the two traffic demands share link l, and then using the indicator $\Delta_{t_1,t_2,h,c}$ to select one XCI PSD value from the lookup table $J^{\text{XCI}}_{t_2,c,h}$. The product of the two variables in (3.49) is equivalent to

$$\begin{aligned}
&n^{\text{XCI}}_{t_1,t_2,l} \leq \theta \cdot \kappa_{t_1,t_2,l}, \\
&n^{\text{XCI}}_{t_1,t_2,l} \leq \sum_{h\in H, c\in M} \Delta_{t_1,t_2,h,c} J^{\text{XCI}}_{t_2,c,h}, \\
&n^{\text{XCI}}_{t_1,t_2,l} \geq \sum_{h\in H, c\in M} \Delta_{t_1,t_2,h,c} J^{\text{XCI}}_{t_2,c,h} + \theta \cdot (\kappa_{t_1,t_2,l} - 1), \\
&n^{\text{XCI}}_{t_1,t_2,l} \geq 0,
\end{aligned} \tag{3.57}$$

for all $(t_1, t_2) \in T^2$ and $l \in E$. Constraint (3.50) calculates the total NLI of a traffic demand by summing up the PSDs of SCI and XCI. It is equivalent to

$$\begin{aligned}
&n^{\text{NLI}}_{t_2,l} \leq \theta \cdot \sigma_{t_2,l}, \\
&n^{\text{NLI}}_{t_2,l} \leq \sum_{c\in M} m_{t_2,c} J^{\text{SCI}}_{t_2,c} + \sum_{t_1:(t_1,t_2)\in T^2} n^{\text{XCI}}_{t_1,t_2,l}, \\
&n^{\text{NLI}}_{t_2,l} \geq \sum_{c\in M} m_{t_2,c} J^{\text{SCI}}_{t_2,c} + \sum_{t_1:(t_1,t_2)\in T^2} n^{\text{XCI}}_{t_1,t_2,l} + \theta \cdot (\sigma_{t_2,l} - 1), \\
&n^{\text{NLI}}_{t_2,l} \geq 0,
\end{aligned} \tag{3.58}$$

for all $(t_1, t_2) \in T^2$ and $l \in E$. Constraint (3.51) imposes that the total noise PSD should be less than the noise tolerance given by the chosen modulation format. And finally, constraint (3.52) calculates the highest index of allocated spectrum slots in the network.

The numbers of variables in the MILP formulation (3.36)–(3.58) are listed in Table 3.1. The total number of variables is $O(|T|^2|S||M|)$. The numbers of linear constraints in (3.36)–(3.52) are listed in Table 3.2. The total number of constraints is $O(|T|^2|E|)$. As can be seen, the number of variables in this MILP formulation is related to the number spectrum slots and, thus, cannot scale very well in large networks. An improved method is proposed in [Paper C] to linearize the nonlinear functions in the GN model and avoid large number indexing variables $\Delta_{t_1,t_2,h,c}$ in look-up tables.

3.5.2 Heuristic Algorithm

The computational complexity of the MILP formulation (3.36)–(3.52) is very high due to the many decision variables and constraints. Therefore, heuristic algorithms have to be used in large scale networks. In [52], the CL method is used to allocate traffic demands one by one. When processing one traffic demand, the estimated NLIs generated from a certain number of future traffic demands are considered together with the previously allocated ones. The traffic demands are assumed to be ordered according to a certain policy, such as descending order of the requested data rates [52].

Table 3.1: The number of variables in the MILP formulation (3.36)–(3.52).

Symbol	Number
f_t	$\|T\|$
δ_{t_1,t_2}	$\|T\|(\|T\|-1)$
$y_{t,i}$	$\|T\|K$
u_{t_1,t_2}	$\|T\|(\|T\|-1)$
ω_{total}	1
$\texttt{spc}(t)$	$\|T\|$
$z_{t,i}$	$\|T\|K$
$m_{t,c}$	$\|T\|\|M\|$
$\Delta_{t_1,t_2,h,c}$	$\|T\|(\|T\|-1)\|S\|\|M\|$
$F^{\text{abs}}_{t_1,t_2}$	$\|T\|(\|T\|-1)$
$\kappa_{t_1,t_2,l}$	$\|T\|(\|T\|-1)\|E\|$
$\sigma_{t,l}$	$\|T\|\|E\|$
$n^{\text{XCI}}_{t_1,t_2,l}$	$\|T\|(\|T\|-1)\|E\|$
$n^{\text{NLI}}_{t,l}$	$\|T\|\|E\|$

Table 3.2: The number of constraints in the MILP formulation (3.36)–(3.52).

Constraints	Number
(3.37)	$\|T\|$
(3.38)	$O(\|T\|K)$
(3.39)	$\|T\|$
(3.40)	$\|T\|\|E\|$
(3.41)	$O(\|T\|(\|T\|-1)\|E\|)$
(3.42)	$\|T\|(\|T\|-1)$
(3.43)	$\|T\|$
(3.44)	$O(\|T\|(\|T\|-1))$
(3.45)	$O(\|T\|(\|T\|-1))$
(3.46)	$\|T\|$
(3.47)	$\|T\|(\|T\|-1)\|M\|$
(3.48)	$O(\|T\|(\|T\|-1))$
(3.49)	$O(\|T\|(\|T\|-1)\|E\|)$
(3.50)	$O(\|T\|\|E\|)$
(3.51)	$\|T\|$
(3.52)	$\|T\|$

3.6 Power Optimization

The NLIs generated in optical networks are closely related to the PSDs of optical connections. By adjusting the PSDs, it is possible to achieve better SNR margins for traffic

demands. Thanks to the NLI expressions provided by the GN model in Section 2.6, simple yet effective PSD optimization rules have been developed to significantly reduce the complexity of control plane algorithms.

One of the well known PSD optimization policies is the local optimum global optimum (LOGO) strategy [53]. Assuming coherent transmission without dispersion compensation, the overall PLI PSD of a connection under test (CUT) can be written as an incoherent accumulation of PLIs from each traversed fiber span

$$G_{\mathrm{Rx}}^{\mathrm{PLI}} = \sum_{n=1}^{N_{\mathrm{span}}} \left(G_n^{\mathrm{NLI}} + G_n^{\mathrm{ASE}} \right), \tag{3.59}$$

where $G_{\mathrm{Rx}}^{\mathrm{PLI}}$ is the PLI PSD per polarization at the receiver of the CUT, N_{span} is the number of spans traversed by the connection, and G_n^{NLI} and G_n^{ASE} are the PSDs of NLI and ASE per polarization produced at the end of the n-th span, respectively. Equation (3.59) assumes that the loss at each span is exactly compensated for by EDFA gains. As a result, the signal PSD of the CUT at the end of each span is the same as the received connection signal PSD. Equation (3.59) can handle nonidentical NLI and ASE noises produced by different fiber types and traffic loads, which are very common in practice. In contrast, (2.11) assumes that fiber links in the network are homogeneous and only calculates PLI per span. According to (2.18), the SNR at the receiver of the CUT can be expressed as

$$\begin{aligned} \mathrm{SNR}_{\mathrm{Rx}} &= \frac{G_{\mathrm{Rx}}}{G_{\mathrm{Rx}}^{\mathrm{PLI}}}, \\ &= \frac{G_{\mathrm{Rx}}}{\sum_{n=1}^{N_{\mathrm{span}}} \left(G_n^{\mathrm{NLI}} + G_n^{\mathrm{ASE}} \right)}, \\ &= \left[\sum_{n=1}^{N_{\mathrm{span}}} \frac{G_n^{\mathrm{NLI}} + G_n^{\mathrm{ASE}}}{G_{\mathrm{Rx}}} \right]^{-1}, \\ &= \left[\sum_{n=1}^{N_{\mathrm{span}}} \frac{1}{\mathrm{SNR}_n} \right]^{-1}, \end{aligned} \tag{3.60}$$

where SNR_n is the SNR of the CUT at the end of the n-th span, due to the NLI and ASE produced exclusively in the n-th span. Equation (3.60) shows that the optimal PSD for a complete path is obtained when the individual SNR in each span is locally maximized.

The LOGO strategy reveals the relation between the local and global optimal SNRs on the link level. In the network scenario, however, the dependence of G_n^{NLI} on the individual connection powers is rather complex since many optical connections can coexist in the same fiber span. To simplify the LOGO strategy, it is assumed that a uniform PSD is used across all the optical connections and the fibers are fully loaded with Nyquist-spaced connections with the same bandwidth. In other words, the rectangular optical connections with uniform PSD and bandwidth are closely packed with zero guardband

in the spectrum. Under these assumptions, the locally produced SNR of the spectrum-central connection at the n-th span is expressed as

$$\begin{aligned} \mathrm{SNR}_{\mathrm{center},n} &= \frac{G_{\mathrm{uniform},n}}{G_n^{\mathrm{NLI}} + G_n^{\mathrm{ASE}}}, \\ &= \frac{G_{\mathrm{uniform},n}}{\varrho_{\mathrm{NLI},n} G_{\mathrm{uniform},n}^3 + G_n^{\mathrm{ASE}}}, \end{aligned} \tag{3.61}$$

where

$$\varrho_{\mathrm{NLI},n} = \frac{3\gamma_n^2}{2\pi\alpha_n|\beta_{2,n}|}\left[2\ln\left(\frac{B_{\mathrm{total}}}{B}\right) + \operatorname{arcsinh}\left(\frac{\pi^2|\beta_{2,n}|}{2\alpha_n}B^2\right)\right], \tag{3.62}$$

$\alpha_n, \beta_{2,n}$, and γ_n are the power attenuation factor, group velocity dispersion coefficient, and nonlinear coefficient of the n-th fiber span, and B_{total} and B are the bandwidth of overall fully loaded spectrum and the central connection, respectively. According to (3.61), the optimal PSD in the n-th fiber span is

$$G_{\mathrm{uniform},n}^{\mathrm{opt}} = \left(\frac{G_n^{\mathrm{ASE}}}{2\varrho_{\mathrm{NLI},n}}\right)^{1/3}. \tag{3.63}$$

The link level PSD optimization in (3.63) that exploits the LOGO strategy under the assumption of a fully loaded spectrum with Nyquist-spaced connections is called the local optimum global optimum Nyquist (LOGON) strategy.

With the LOGON strategy, PSDs can be optimized at different spans with different fiber types. Since only local fiber parameters are needed in the PSD optimization, a static power control system can be deployed at each fiber span independent of the link spectral load. The SNR of a traffic demand is simply estimated with (3.60) and (3.61). When new traffic demands arrive in the network, the SNRs of the existing traffic demands do not need to be estimated again since the LOGON strategy is based on the fully loaded spectrum. This allows agile and robust reconfiguration of optical networks with guaranteed satisfactory QoTs [54].

Note that other power optimization algorithms considering the interaction between all the traffic demands also exist. For example, a uniform PSD for all the connections can be optimized in [52] by sweeping the PSD value within a range and allocating resource repeatedly. The optimal PSD is selected after the sweeping procedure. Individual PSD can be optimized in [Paper C] together with the routing, spectrum, and modulation assignment. Compared to the LOGON strategy, the solutions of these power allocation algorithms are closer to the optima at the cost of higher computational burden on the control plane of the network. Whereas the LOGON strategy offers a simpler power control scheme in heavily loaded networks with heterogeneous fiber links.

Chapter 4

Regenerator Location Problem

In long-haul optical networks, the distances between the sources and destinations of some of the traffic demands can be longer than the transmission reach of any available modulation format. Consequently, direct transmission of optical signals is impossible. It is necessary to deploy one or more optoelectronic regenerators along the route of traffic demands to restore optical signals.

We start by introducing the regeneration techniques in Section 4.1. In Section 4.2 we outline the generic regenerator location problem (RLP) in WDM networks, which assigns routes and wavelengths to traffic demands and RSs to network nodes. The routing-constrained RLP is reviewed in Section 4.3. In Section 4.4, the RLP in flexible-grid optical networks is briefly described. Finally, the RLP considering time-varying traffic is motivated in Section 4.5.

4.1 Regeneration in Optical Networks

In Chapter 3, the resource allocation algorithms assume totally transparent networks where any traffic demand can be transmitted from its source to destination with QoT satisfied. This is the case for networks with relatively small geographic range or low-noise amplifiers. For current large scale networks, however, regeneration is still necessary to guarantee the quality of each traffic demand.

The regenerator is based on optical-electrical-optical (O-E-O) technology, which consists of a pair of back-to-back transponders. It first converts incoming optical signal to electrical bits, and then converts them back to the optical domain. The process of O-E-O conversion reamplifies, reshapes, and retimes the signal and, thus, called 3R regeneration. Usually, regenerators are also quipped with tunable lasers so that the wavelength of optical signals can also be changed after regeneration. Optionally, regenerators are possible to provide FEC decoding, dispersion compensation, and optical performance monitoring capacity to enhance QoTs and extend TRs [55, 56].

Due to the structure of regenerators, costs comparable to a pair of transponders is added to the network. Therefore, it is desirable to reduce the number of regenerators

in the network. Regenerators also require costly manual setup and maintenance, hence it is preferred to concentrate them in a few network nodes, known as regenerator sites (RSs). Whether an optical connection needs regeneration or not depends on its particular transmission parameters and PLIs. As a result, to achieve the best resource usage, regenerators can be jointly allocated together with other resources in the network [15, 21]. On the other hand, estimation of future traffic demands is required to solve this joint optimization. Therefore, from the network operator's viewpoint, the joint allocation can be carried out if the future traffic pattern is static or predictable at the early stage of the network construction, whereas a separate optimization of RSs is more reasonable if time-varying traffic is present. In the second case, efficient resource usage and good network performance can be achieved by combining the knowledge of the traffic pattern with RS placements [Paper D].

4.2 RLP in WDM Networks

To achieve a cost-effective network design, it is important to properly allocate RSs such that their total number is minimized. The RSs should ensure that the QoT requirements of all traffic demands are satisfied. Here, the routing and wavelength assignment is also considered in the RS placement problem to achieve efficient utilization of regenerators. The RLP can be stated as

- *Inputs*: the network topology and set of traffic demands.
- *Outputs*: the selected RSs, routes, and wavelengths allocated to all the traffic demands.
- *Constraints*: all the traffic demands should have satisfactory QoTs, which is measured by the TR model.
- *Objective*: minimize the total network cost.

The RWA in Section 3.2 can be considered as a special case of the RLP with fixed RS placement. Therefore, the RLP is at least as hard as the RWA and involves high computational complexity for large scale optical networks. For the sake of simplicity, the TR model is used in the QoT constraint and only one modulation format is available in the network.

The network topology is denoted as $G = (V, E)$, where V is the set of nodes and E is the set of links. Each link has two fibers with opposite directions. The first step of solving the RS placement problem is to construct an *augmented network* $G_A = (V_A, E_A)$ based on the original network G in the following steps [15, 57]:

1. Copy all nodes from the original network G into the augmented network G_A, i.e., $V_A = V$.
2. Connect two nodes u and v in the augmented network with two auxiliary links with opposite directions if there exists a route between u and v in G with length less than the transmission distance of the available modulation format.

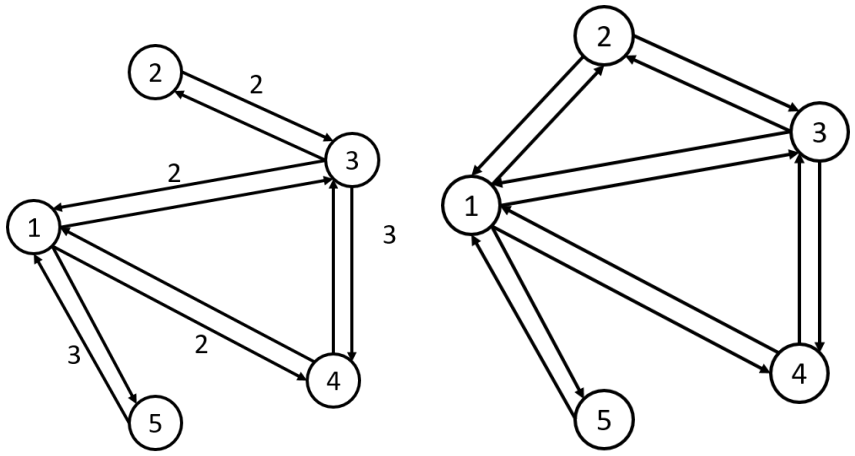

Figure 4.1: The original and augmented graphs for the RLP. (a): Original network G; the number on edges are link lengths in number of fiber spans; (b): Augmented graph G_A, two directional link between the neighbor pair $(1, 2)$ is included. The TR is 4 fiber spans here.

We say that nodes u and v form a *neighbor pair* (u, v) if they are connected in G_A. For each neighbor pair (u, v), there exists at least one route in G connecting them without signal regeneration. This route is called the *component set* of the neighbor pair (u, v). If two nodes are not a neighbor pair, then regeneration is necessary for connecting them. With a slight abuse of notation, we also use the neighbor pair (u, v) to denote the link in G_A connecting nodes u and v.

Figure 4.1 illustrates the concept of the augmented graph. In Fig. 4.1(a), link lengths in number of fiber spans are indicated by numbers on the edge of the original graph G. Assuming a TR of 4 fiber spans, two links with opposite directions connecting nodes 1 and 2 are included in Fig. 4.1(b) because they form a neighbor pair. Actually, the route $1 - 3 - 2$ connects nodes 1 and 2 without violating the transmission distance. There are no other neighbor pairs in this graph.

A problem equivalent to the RLP in G can be formulated in G_A. For a connection between two nodes which are not a neighbor pair, we need to find a route in G_A, and place RSs on each intermediate node on the route. The objective of the RS placement problem is thus converted to minimizing the total number of intermediate nodes in G_A.

Based on the observation above, an ILP can be formulated for the RLP. The input parameters of the ILP formulation are

- $G_A = (V_A, E_A)$: the augmented network, where V_A is the set of nodes and E_A is the set of directional links in G_A.
- W: the set of wavelengths on the fiber links.

- T: The set of traffic demands, each demand $t \in T$ is represented by its source $\texttt{src}(t)$ and destination $\texttt{dst}(t)$. Since our focus in the RLP problem is to allocate RSs, we assume that each traffic demand requests only one wavelength for the sake of simplicity.
- E_v^+: the set of directional links in G_A that go out from node $v \in V$.
- E_v^-: the set of directional links in G_A that go into node $v \in V$.
- $\texttt{com}(u, v)$: A precalculated component set of neighbor pair $(u, v) \in E_A$. I.e., it is an ordered set of links connecting nodes u and v in G. In the case where multiple component sets are found, arbitrary one is selected.

Note that E_v^+ and E_v^- are equivalent to the sets of neighbor pairs of node v in G_A instead of physical links in G. The decision variables in the ILP formulation are listed below.

- $r_v \in \mathbb{B}$: equals 1 if an RS is placed on node $v \in V$, and 0 otherwise.
- $f_{u,v,w}^t \in \mathbb{B}$: equals 1 if wavelength $w \in W$ on link $(u, v) \in E_A$ is used by the traffic demand $t \in T$, and 0 otherwise.

The ILP formulation of the RS placement problem can be expressed as [57]

$$\text{minimize} \quad w_{\text{total}} + \sum_{v \in V} r_v \tag{4.1}$$

$$\text{subject to} \quad \sum_{v \in E_u^-} \sum_{w \in W} f_{v,u,w}^t = 0, \qquad \forall t \in T, u = \texttt{src}(t), \tag{4.2}$$

$$\sum_{v \in E_u^+} \sum_{w \in W} f_{u,v,w}^t = 1, \qquad \forall t \in T, u = \texttt{src}(t), \tag{4.3}$$

$$\sum_{v \in E_u^+} \sum_{w \in W} f_{u,v,w}^t = 0, \qquad \forall t \in T, u = \texttt{dst}(t), \tag{4.4}$$

$$\sum_{v \in E_u^-} \sum_{w \in W} f_{v,u,w}^t = 1, \qquad \forall t \in T, u = \texttt{dst}(t), \tag{4.5}$$

$$\sum_{v \in E_u^+} f_{u,v,w}^t = \sum_{v \in E_u^-} f_{v,u,w}^t, \qquad \begin{array}{l} \forall t \in T, w \in W, \\ u \in V, u \neq \texttt{src}(t), \texttt{dst}(t), \end{array} \tag{4.6}$$

$$\sum_{t \in T} f_{u,v,w}^t \leq 1, \qquad \forall w \in W, (u, v) \in E_A \tag{4.7}$$

$$\sum_{t \in T} f_{u,v,w}^t + \sum_{t \in T} f_{m,n,w}^t \leq 1, \qquad \begin{array}{l} \forall w \in W, (u, v) \in E_A, \\ (m, n) \in \texttt{com}(u, v) \end{array} \tag{4.8}$$

$$r_u \geq \sum_{v \in E_u^+} f_{u,v,w}^t, \qquad \begin{array}{l} \forall w \in W, t \in T, u \in V, \\ u \neq \texttt{src}(t), \texttt{dst}(t), \end{array} \tag{4.9}$$

$$w_{\text{total}} \geq w \sum_{t \in T} f_{u,v,w}^t, \qquad \forall w \in W, (u, v) \in E_A. \tag{4.10}$$

The objective is to minimize the total network cost including the number of RSs and the number of wavelengths used to establish all the connections. Constraints (4.2)–(4.6) are the flow conservation constraint. Constraints (4.7) and (4.8) ensure that no two traffic demands can share the same wavelength on the same link. Constraint (4.9) assigns RS to intermediate nodes on the route of any connection in the augmented network. Constraint (4.10) calculates the highest wavelength index used by all the links.

The total number of variables in the ILP formulation (4.1)–(4.10) is dominated by the variable $f^t_{u,v,w}$ and, thus, equals $O(|W||V|^2|T|)$. The number of constraints (4.2)–(4.5) is $4|T|$, the number of constraints (4.6) is approximately $|T||W||V|$, the number of constraints (4.7) is $O(|W||V|^2)$, the number of constraints (4.8) is $O(|W||V|^4)$, the number of constraints (4.9) is $O(|T||W||V|)$, and the number of constraints (4.10) is $O(|W||V|^2)$. Consequently, the total number of constraints is $O(|W||V|^4 + |T||W||V|)$.

4.3 Routing-Constrained RLP

The classic RLP in Section 4.2 only minimizes the total number of RSs, leaving the routes of individual traffic demands unconstrained. In reality, however, the transmission latency is also an important criterion and should be considered when allocating routes to traffic demands. Therefore, it is beneficial to consider a broader definition of the cost model by including the length of the route as well as the regenerator count. The cost of a route p can be defined as [15]

$$\texttt{cost}(p) = c_r \times R(p) + c_m \times L(p), \tag{4.11}$$

where $\texttt{cost}(p)$ is the overall cost of route p, $R(p)$ is the number of regenerators in route p, $L(p)$ is the length of route p in kilometer, c_r is the cost per regenerator, and c_m is the cost of route per kilometer. For example, if we set $c_r = 1$ and $c_m = 0$, only the number of RSs is considered when selecting routes. Whereas if $c_r = 0$ and $c_m = 1$, the traffic demands are delay sensitive and should use the minimum distance routes.

Based on the cost model in (4.11) the routing-constrained RLP problem is stated as

- *Inputs:* The network topology, set of traffic demands, and specific cost model.
- *Outputs:* the selected RSs.
- *Constraints:*
  1. *QoT constraint:* the transmission distance of the available modulation format is not violated.
  2. *Routing constraint:* cost-effective routes are used for all the traffic demands.
- *Objective:* minimize the overall network cost, which is the total cost of all traffic demands.

To search for cost-effective routes, the augmented network $G_A = (V_A, E_A)$ needs to be modified such that each link $l \in E_A$ is also associated with a weight η_l expressed as

$$\eta_l = c_r + c_m \times L_l, \tag{4.12}$$

where L_l is the length of the route connecting the source and destination nodes of l in G. Based on the link weight in (4.12), the cost of the route p connecting nodes u and v in G_A is rewritten as

$$\begin{aligned} \texttt{cost}(p) &= c_r \times R(p) + c_m \times L(p), && (4.13)\\ &= c_r \times (|p| - 1) + c_m \times \sum_{l \in p} L_l, && (4.14)\\ &= \sum_{l \in p} (c_r + c_m \times L_l) - c_r, && (4.15)\\ &= \sum_{l \in p} \eta_l - c_r. && (4.16) \end{aligned}$$

Here (4.13) is the definition of the route cost. Since the route p is an ordered set of links connection u and v in G_A, $|p| - 1$ is the number of intermediate nodes (and equivalently the number of RSs) on it. And the length of route p equals the sum of each link in p. Therefore, we have $R(p) = |p| - 1$ and $L(p) = \sum_{l \in p} L_l$ in (4.14). Equation (4.15) rewrites (4.14) and leads to the route cost in (4.16), according to which cost-effective routes can be found by searching for the shortest paths in G_A.

So far, we assume that the minimum-cost routes are used for all the traffic demands. However, the total number of RSs can be further reduced if we allow the algorithm to pick routes that are slightly more costly for some of the traffic demands [15]. To this end, we can apply a latitude L_t to traffic demand $t \in T$ to allow it to pick any route that is of cost within $1 + L_t$ of the minimum-cost route. It is reasonable to assign small or zero latitudes to important traffic demands and larger latitudes to less prioritized ones.

The input parameters of the ILP formulation of routing-constrained RLP are

- $G_A = (V_A, E_A)$: The weighted augmented network, where V_A is the set of nodes and E_A is the set of directional links. Each link l in E_A is associated with a cost η_l expressed in (4.12).
- W: the set of wavelengths on the fiber links.
- T: the set of traffic demands, each demand $t \in T$ is represented by its source $\texttt{src}(t)$ and destination $\texttt{dst}(t)$.
- E_v^+: the set of directional links in G_A that go out from node $v \in V$.
- E_v^-: the set of directional links in G_A that go in to node $v \in V$.
- $\texttt{com}(u, v)$: the component set of neighbor pair $(u, v) \in E_A$.
- $H_t \in \mathbb{R}_+$: the cost of the shortest route in G_A that connects $\texttt{src}(t)$ and $\texttt{dst}(t)$ for $t \in T$.
- $\eta_{u,v}$: the cost of the link $(u, v) \in E_A$.
- $L_t \in \mathbb{R}$: the latitude assigned to traffic demand $t \in T$.

The decision variables in the ILP formulation are listed below

- $r_v \in \mathbb{B}$: equals 1 if RS is placed on node $v \in V$, and 0 otherwise.
- $f^t_{u,v,w} \in \mathbb{B}$: equals 1 if wavelength $w \in W$ on link $(u, v) \in E_A$ is used by the traffic demand $t \in T$, and 0 otherwise.

The ILP formulation of the routing-constrained RS placement problem can be expressed as [15, 57]

$$\text{minimize} \quad w_{\text{total}} + \sum_{v \in V} r_v \tag{4.17}$$

$$\text{subject to} \quad \sum_{v \in E_u^-} \sum_{w \in W} f^t_{v,u,w} = 0, \qquad \forall t \in T, u = \texttt{src}(t), \tag{4.18}$$

$$\sum_{v \in E_u^+} \sum_{w \in W} f^t_{u,v,w} = 1, \qquad \forall t \in T, u = \texttt{src}(t), \tag{4.19}$$

$$\sum_{v \in E_u^+} \sum_{w \in W} f^t_{u,v,w} = 0, \qquad \forall t \in T, u = \texttt{dst}(t), \tag{4.20}$$

$$\sum_{v \in E_u^-} \sum_{w \in W} f^t_{v,u,w} = 1, \qquad \forall t \in T, u = \texttt{dst}(t), \tag{4.21}$$

$$\sum_{v \in E_u^+} f^t_{u,v,w} = \sum_{v \in E_u^-} f^t_{v,u,w}, \qquad \begin{array}{l}\forall t \in T, w \in W, \\ u \in V, u \neq \texttt{src}(t), \texttt{dst}(t),\end{array} \tag{4.22}$$

$$\sum_{t \in T} f^t_{u,v,w} \leq 1, \qquad \forall w \in W, (u, v) \in E_A \tag{4.23}$$

$$\sum_{t \in T} f^t_{u,v,w} + \sum_{t \in T} f^t_{m,n,w} \leq 1, \qquad \begin{array}{l}\forall w \in W, (u, v) \in E_A, \\ (m, n) \in \texttt{com}(u, v)\end{array} \tag{4.24}$$

$$r_u \geq \sum_{v \in E_u^+} f^t_{u,v,w}, \qquad \begin{array}{l}\forall w \in W, t \in T, u \in V, \\ u \neq \texttt{src}(t), \texttt{dst}(t).\end{array} \tag{4.25}$$

$$\sum_{(u,v) \in E_A} \eta_{u,v} \sum_{w \in W} f^t_{u,v,w} - c_r \leq (1 + L_t) H_t, \qquad \forall t \in T, \tag{4.26}$$

$$w_{\text{total}} \geq w \sum_{t \in T} f^t_{u,v,w}, \qquad \forall w \in W, (u, v) \in E_A. \tag{4.27}$$

The only difference between the ILP formulation (4.17)–(4.27) and (4.1)–(4.10) is the inequality (4.26), which requires the cost of the selected route to be within $1 + L_t$ of the minimum-cost route of t.

4.4 RLP in Flexible-Grid Networks

The RLP in flexible-grid networks also needs to assign routing and spectrum to traffic demands. Therefore, its complexity is very high. For the sake of simplicity, the problem is

decomposed into two subproblems and solved sequentially. The first subproblem assigns routing and RSs and the second subproblem allocates spectrum resources.

Similar to the problems in Sections 4.2 and 4.3, the routing and RS assignment subproblem can be solved as an ILP problem. The input parameters of the ILP formulation are

- $G_A = (V_A, E_A)$: the augmented network, where V_A is the set of nodes and E_A is the set of directional links in G_A.
- T: The set of traffic demands, each demand $t \in T$ is represented by its source $\texttt{src}(t)$ and destination $\texttt{dst}(t)$.
- E_v^+: the set of directional links in G_A that go out from node $v \in V$.
- E_v^-: the set of directional links in G_A that go into node $v \in V$.

The variables in the ILP formulation are

- $f_{u,v}^t \in \mathbb{B}$: equals 1 if the neighbor pair $(u, v) \in E_A$ is used to traffic demand $t \in T$, and 0 otherwise.
- $r_v \in \mathbb{B}$: equals 1 if the node $v \in V$ is selected as an RS, and 0 otherwise.

The ILP formulation of the routing and RS assignment subproblem is

$$\text{minimize} \quad \sum_{v \in V} r_v \tag{4.28}$$

$$\text{subject to} \quad \sum_{v \in E_u^+} f_{u,v}^t - \sum_{v \in E_u^-} f_{v,u}^t = \begin{cases} 0, & u \neq \texttt{src}(t), \texttt{dst}(t), \\ 1, & u = \texttt{src}(t), \\ -1, & u = \texttt{dst}(t), \end{cases} \quad \forall u \in V, t \in T, \tag{4.29}$$

$$r_u \geq \sum_{v \in E_u^+} f_{u,v}^t, \quad \forall t \in T, u \in V, \; u \neq \texttt{src}(t), \texttt{dst}(t). \tag{4.30}$$

The objective is to minimize the total number of RSs. Equation (4.29) is the flow conservation constraint. Constraint (4.30) assigns RS to intermediate nodes on the route of any traffic demand in the augmented network. Optionally, the following constraint

$$\sum_{(u,v) \in E_A} \eta_{u,v} f_{u,v}^t - c_r \leq (1 + L_t) H_t, \quad \forall t \in T, \tag{4.31}$$

can be added to the ILP formulation to select only cost-effective routes.

The spectrum allocation subproblem can be solved by the CL method presented in Section 3.5.2. The traffic demands are first sorted according to certain policy, such as the descending order of data rate [52]. After that, the spectrum slots are assigned to the traffic demands one by one using the first-fit method [49]. Since RSs are allocated in the network, the spectrum continuity constraint only applies to the route segments between consecutive RSs on the route of a connection.

4.5 RLP with Time-Varying Traffic

The optical networks discussed so far in Chapters 3 and 4 have static traffic demands. This is the case when optical components are inflexible and traffic patterns are predictable. However, as reconfigurable optical components mature and services tend to be more dynamic in recent years, variable traffic demands become realistic gradually [41, p. 349]. For example, bandwidth-variable wavelength crossconnects (BV-WXCs) and bandwidth-variable transceivers (BV-Ts) will enable the network operators to dynamically change the bandwidth of optical connections according to real-time communication requirements and achieve cost-effective and highly available connectivity [8]. The time-varying services can be data backup service of DCs during night hours, video-on-demand services of individual users during evening hours, and transaction data between financial institutes during working hours [58].

In such network scenario, the resource allocation algorithms should take into account the variable nature of traffic demands. It has been shown that more requested data rates can be provisioned by multihour RSA with predicted traffic demands [58] and real-time bandwidth adjustment [59]. Moreover, network utilization and service availability can be improved with online defragmentation and spectrum reoptimization [60]. These adaptive resource allocation strategies imply constantly changing bandwidths, carrier frequencies, and spectral spacings of optical connections, whose resultant NLIs are also time-varying and difficult to mitigate. On the other hand, if allocated properly, RSs can compensate for the stochastic NLIs and provide robust and satisfactory QoTs.

In [Paper D], we studied the RLP in flexible-grid optical networks with time-varying traffic. The route for every connection is precalculated using the cost model in Section 4.3 and method in Section 4.4. Then statistical network assessment process [61, 62] is performed to estimate distributions of NLIs for each connection on its route, based on which RSs are selected to minimize the expected traffic blocking.

Chapter 5

Data Center Networks

In modern data centers (DCs), there are a large number of computing and storage servers, which are interconnected by a specially designed network, namely, a data center network (DCN). Optical communication has been introduced in DCNs as a promising solution offering high throughput and low power consumption.

In Section 5.1, we briefly introduce the traditional DCNs architecture. The optical switching techniques used in DCNs are outlined in Section 5.2. The resource allocation algorithms involved in the optical DCNs are described in Section 5.3.

5.1 Traditional DCNs

DC is one of the major infrastructures of Internet. It usually hosts a large number of computing and storage resources that communicate extensively with each other [63]. The interconnection of such vast amount of servers is not trivial and, thus, requires sophisticated design of DCNs.

Figure 5.1 illustrates a tree-like architecture [64], which is typical in traditional DCNs [65]. At the bottom of the architecture, servers from the lowest hierarchy are organized into server racks consisting of 40 to 80 blades. Each blade server is connected to a Top-of-Rack (ToR) switch. At the intermediate tier, ToR switches are connected to aggregate switches. Moving up the architecture, the traffic from aggregate switches is consolidated further in core switches. One aggregate switch is connected to more than one core switches for redundancy. At the top tier, core switches provide connectivity between all the servers inside the DC and the content switches[1] are used to route requests from users to appropriate servers inside the DC.

DCNs illustrated in Fig. 5.1 are mainly placed in fixed locations. As DCs are developing fast, they should be easy to deploy and upgrade to satisfy the flexible requirements [66]. The concept of modular DC (MDC) has been proposed, which is placed in a shipping-based container referred to as performance optimized DC (POD) [67]. Each

[1]Content switch directs incoming traffic according to their contents. Therefore, load balance across multiple servers can be performed based on the availability of contents and loads on servers.

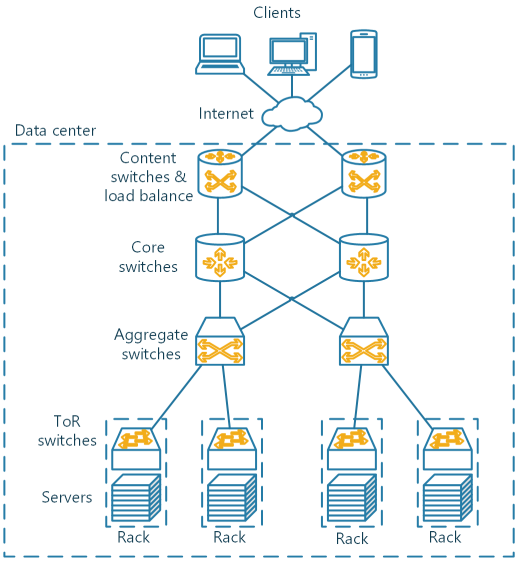

Figure 5.1: Illustration of a typical DCN architecture.

POD is a small DC that includes hundreds to thousands of servers, storage devices, network devices, and power and cooling systems. It is flexible to run one POD independently or connect multiple of them to build a larger MDC. Therefore, the MDC is considered as an effective solution to build and maintain large DC facilities.

The tree-like DCN and MDC mentioned above are traditionally based on electrical switches and cables. Therefore, their power consumption and cabling complexity are very high due to the many electrical devices and links. Another problem is the low network throughput limited by the high-cost electrical devices, which cannot support high data rate communication easily. Moreover, the size of DCs is constantly growing driven by increasing demands for various applications. As a result, the throughput in the future DCN must be improved significantly to sustain the increased network traffic. While the performance requirement of DCs will increase rapidly in the next few years, the total affordable power consumption of DCs grows at a much slower rate due to thermal dissipation and economic considerations [64].

5.2 Optical Interconnects in DCNs

To improve the performance and reduce the power consumption simultaneously, it is important to select the appropriate switching and transmission technology in DCNs. Optical communication is a promising solution to the networking problems in traditional DCNs. Its advantages include

- **High capacity:** By using WDM or flexible-grid techniques in optical communica-

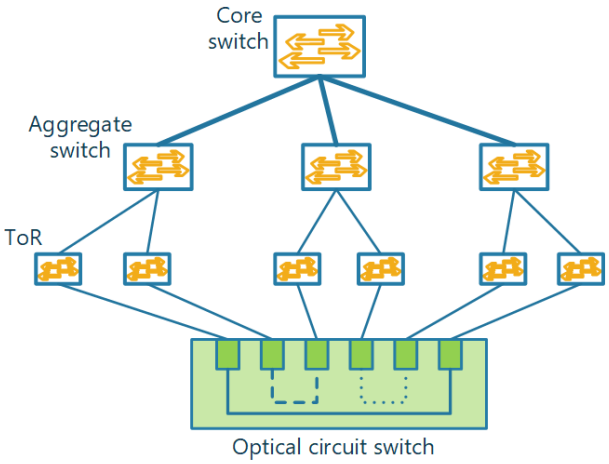

Figure 5.2: Architecture of the c-Through network. All the switches are electrical except the optical circuit switch.

tion, it is possible to transmit multiple optical connections in parallel in the same fiber. Each optical connection can easily achieve a data rate of 100 Gbps. This can be used to connect the large number of servers inside DCs and provide high bandwidth. Additionally, the cabling complexity and space usage of DCNs can be reduced significantly.

- **Low power consumption:** One of the major characteristics of optical links and switches is low power consumption. The low transmission loss of optical fibers allows very long intra-DC links without the need for regeneration. Moreover, the power consumption of optical switches is independent of the bandwidth of optical signals thanks to the wavelength routing technique. Hence, the power per unit bandwidth in optical switches is much lower than that of electrical switches.

The first step of applying optical switching in DCN is to complement conventional electrical switching. As the traffic aggregates more in the hierarchy, long-lived flows with high data rates tend to be more common. Consequently, it becomes beneficial to use optical switches at the top tier of DCNs to connect the core and aggregate switches in Fig. 5.1. In the following, a few DCN architectures based on optical switching are briefly introduced.

5.2.1 C-Through: Part-Time Optics in DC

As illustrated in Fig. 5.2, the c-Through architecture [68] is based on a tree-like topology. The ToR switches are connected both to an electrical packet switching network and an optical circuit-based network. The optical circuit-switching network can only provide a matching between ToRs, i.e., each ToR can be connected to at most one other ToR.

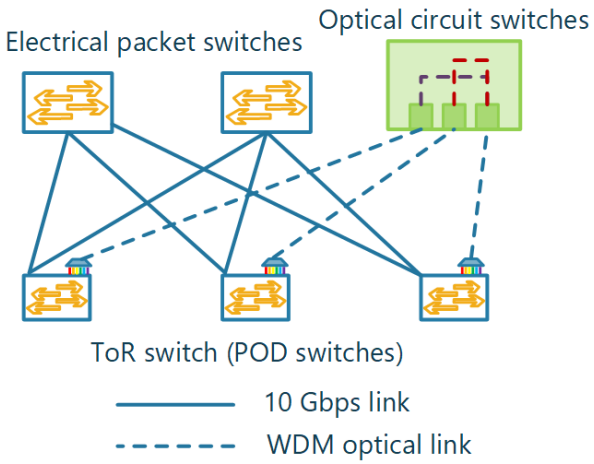

Figure 5.3: Architecture of the Helios network.

Small traffic flows are directed to the electrical packet switching network, whereas large traffic flows go through the optical circuit switching network. An optical configuration manager is used to collect the bandwidth requirements, based on which the configuration of the optical switch is determined. The matching between ToRs in the optical switch can be formulated as a maximum weight matching problem [68]. It has been shown that for applications with slowly changing traffic demands between racks, the c-Through architecture can reduce significantly the time used to establish traffic demands [64].

5.2.2 Helios: A Hybrid Optical Electrical Switch

Helios is a hybrid optical electrical switch architecture for MDC. As is shown in Fig. 5.3, it connects POD switches using both electrical packet switches and optical circuit switches with WDM links. The electrical packet switches are used for all-to-all communication of PODs, while slowly-changing traffic with high bandwidth requests use the optical circuit switches. Similar to c-Through, the optical circuit switch in Helios can only connect pairs of PODs. Helios computes an optical path configuration based on the traffic demands using maximum weight matching [69]. Then the configuration of optical connections is sent to the electrical switches and micro-electro-mechanical systems (MEMS) inside the optical circuit switch to route signals accordingly.

The advantage of Helios is that it is built on readily available optical modules and transceivers that are extensively used in optical communication networks. The drawback of Helios is the long reconfiguration time of the MEMS switch, which is based on mechanical systems to physically rotate mirror arrays. Hence any reconfiguration of the optical circuit switch needs several milliseconds. Therefore, Helios is good for applications where the connections between some nodes last more than a few seconds in order

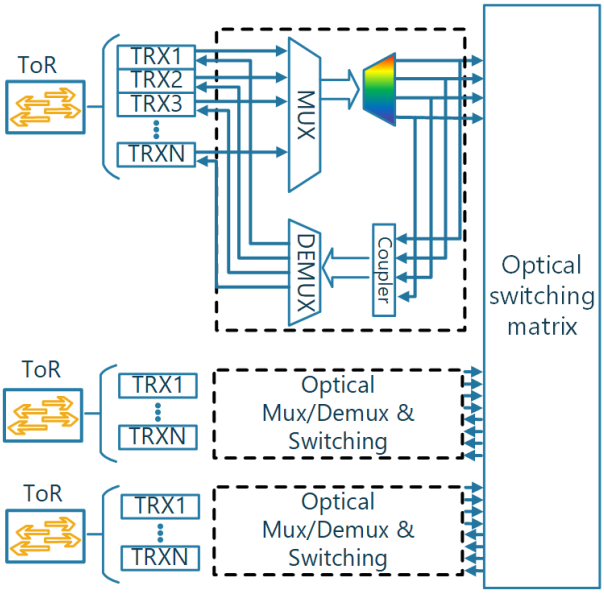

Figure 5.4: Architecture of the Proteus network.

to compensate for the reconfiguration overhead [64].

5.2.3 Proteus: All-Optical DCN Architecture

The architectures mentioned above both aim at enhancing the DCN with complementary optical circuit switching networks. In contrast, Proteus [70] is proposed as an all-optical architecture fully based on optical components and switches. It combines both wavelength-selective switching (WSS) and space switching to increase switching granularity and enables connections from each ToR to multiple other ToRs simultaneously. In Proteus, each ToR switch is equipped with several optical transceivers using unique wavelengths for sending and receiving data. These wavelengths are combined using a multiplexer and routed to a WSS. The WSS is able to switch an arbitrary number of wavelengths to each of its k output ports, which are connected to a MEMS switch that establishes connections among ToRs and enables their connectivity through one or multiple wavelengths. Note that each ToR is connected to k other ToRs and, thus, multiple-hop routing is employed for network connectivity.

Proteus uses direct optical connections between ToRs with high-volume traffic demands and multiple-hop connections for low-volume ToR pairs. The advantage of Proteus is the flexibility of bandwidth and network topology. Proteus can choose an arbitrary topology from a large class of graphs (connected k-regular graphs) and vary the capacity of the links [70], whereas Helios and c-Through can only provide a limited number of single-hop optical links with fixed capacity. The main challenge of Proteus is to find

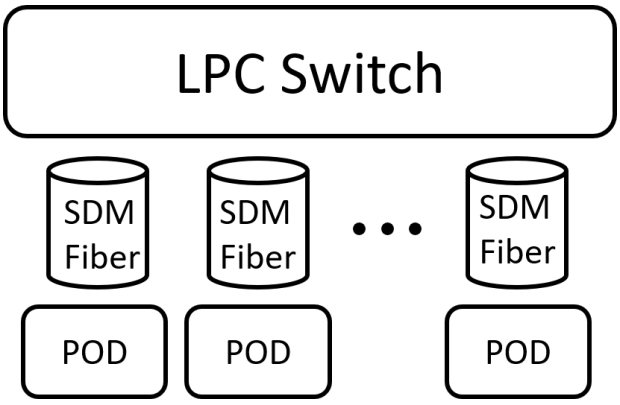

Figure 5.5: Architecture of the SDM-based DCN.

the optimum configuration for the optical switches. An ILP is used to optimize the configuration for given traffic demands.

5.2.4 SDM-Based DCNs

In the above-mentioned architectures, commercial optical circuit switches are used to improve capacity of DCNs. However, the PODs in future MDC can contain thousands of blade servers, each equipped with network interface cards with 10 Gbps or higher capacity. The resultant traffic generated by each POD is on the order of several Tbps and, thus, cannot be satisfied by commercial optical circuit switches. Consequently, future MDC will require networks with ultrahigh capacity and low cabling complexity to interconnect the PODs [24]. However, the conventional optical DCN architectures cannot provide a good solution to future MDCs due to the intrinsic limitation imposed by the underlying optical devices.

Optical SDM is a promising solution to increase fiber transmission capacity. Based on optical fibers with multiple spatial elements, e.g., multimode, multicore, or multielement fibers [71], SDM arranges signals in the spatial domain to improve transmission capacity and reduce cabling complexity. The topology of SDM based DCNs for MDCs is shown in Fig. 5.5. The PODs are connected to each other through a single optical large port count (LPC) spatial switch. Each POD is connected to the LPC switch with a single bidirectional SDM fiber that supports both spatial and spectral multiplexing.

As illustrated in Fig. 5.6, there are different ways of multiplexing signals in the spectral and spatial domains of SDM fibers [24]. In the first scheme, which is referred to as *uncoupled SDM with spectral flexibility*, multiple independent spectral connections can be established. Its resource multiplexing diagram is shown in Fig. 5.6(a), where each of the spatial element operates as an independent flexible-grid fiber. The second secheme is referred to as *coupled SDM with spectral flexibility*, which is shown in Fig. 5.6(b). This switching scheme expands spectral connections to all the spatial elements to create

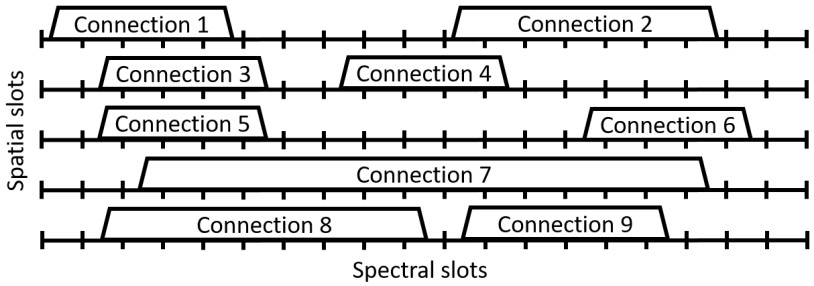

(a) Uncoupled SDM with spectral flexibility

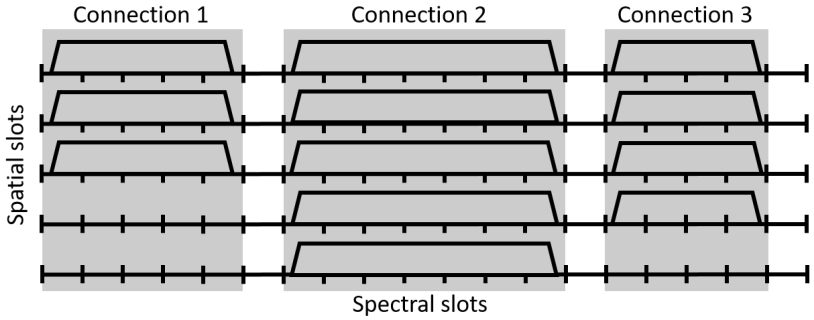

(b) Coupled SDM with spectral flexibility

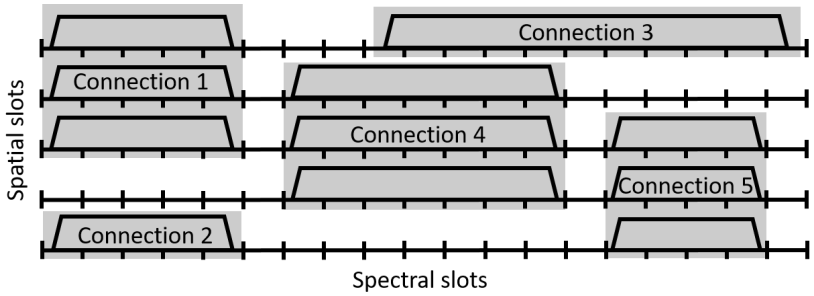

(c) Coupled SDM with spectral and spatial flexibility

Figure 5.6: The different SDM switching schemes.

spectral–spatial connections with increased capacity. Figure 5.6(c) illustrates the *coupled SDM with spectral and spatial flexibility*. Here, unrestricted flexibility in both spectral and spatial domains are exploited to form flexible spectral–spatial connections.

5.3 Resource Allocation in Optical DCNs

To fully exploit the advantages of the optical DCNs, we need to properly configure optical switches according to traffic demands. In this section, the resource allocation problems related to the optical DCN architectures in Section 5.2 are briefly discussed.

5.3.1 Maximum Weighted Matching in C-Through and Helios

In c-Through [68] and Helios [69], the MEMS switches are reconfigured every time the data rates of traffic demands change. The goal of the reconfiguration is to maximize the throughput of the optical switching network. Due to the structure of the optical switch, one POD (ToR) can only be connected to exactly one other POD (ToR) [68, 69].

The configuration of optical switches is a maximum weight matching problem. Given the traffic demands between PODs (ToRs), an undirected weighted graph $G = (V, E)$ can be constructed, where each node $v \in V$ represents one POD (ToR) and each link $(u, v) \in E$ is associated with a weight $w_{u,v}$ equals the requested data rate between u and v for $u, v \in V$. Note that since G is undirected, links (u, v) and (v, u) are identical and, thus, only one of them needs to be considered. A matching M in G is a set of pairwise nonadjacent links. In other words, no two links share a common node. A simple ILP can be formulated to better understand the problem. In this ILP, a decision variable $x_{u,v} \in \mathbb{B}$ for all $(u, v) \in E$ is used, where $x_{u,v} = 1$ if a connection is established between u and v, and 0 otherwise.

$$\text{maximize} \quad \sum_{(u,v)\in E} w_{u,v} x_{u,v} \tag{5.1}$$

$$\text{subject to} \quad \sum_{\substack{v\in V:\\ (u,v)\in E}} x_{u,v} \leq 1, \qquad \forall u \in V. \tag{5.2}$$

Objective (5.1) calculates the aggregated weight and constraint (5.2) ensures the solution is a matching in G. In practice, the solution of the maximum weighted matching problem can be computed in polynomial time by the blossom algorithm [72, 73].

5.3.2 Network Configuration in Proteus

The resource allocation in Proteus involves: a) MEMS configuration to adjust the overall optical network topology and provide high network throughput, b) WSS configuration for each ToR to provision its wavelengths and links, and c) routes between ToR-pairs to achieve high throughput [70]. Similar to c-Through and Helios, the data rates of traffic demands are assumed to be known. The problem can be stated as follows:

- *Input:* the set of traffic demands.
- *Output:* the configuration of the MEMS, WSSs, and wavelengths.
- *Constraints:*

1. each ToR can use one wavelength to connect to at most one other ToR.
2. the number of connections established per ToR is limited by the number of ports per WSS.
3. traffic flow conservation is satisfied at each ToR.

- *Objective:* maximize the overall established data rate.

Based on the problem statement, an MILP can be formulated to solve the network configuration problem. The input parameters to the MILP are

- T: the set of ToRs.
- $D_{i,j} \in \mathbb{R}_+$: The data rate from ToRs i to j for $i, j \in T, i \neq j$.
- $W \in \mathbb{Z}_+$: the number of ports per WSS.
- Λ: the set of available wavelengths.
- $C_{\text{port}} \in \mathbb{R}_+$: the maximum data rate of one WSS port.
- $C_\lambda \in \mathbb{R}_+$: the maximum data rate of one wavelength.

The variables in the MILP are

- $l_{i,j} \in \mathbb{B}$: equals 1 if ToR i is directly connected to ToR j through the MEMS, and 0 otherwise, $i, j \in T, i \neq j$.
- $w_{i,j,k} \in \mathbb{B}$: equals 1 if ToR i is directly connected to ToR j through the MEMS using wavelength λ_k, and 0 otherwise, $i, j \in T, i \neq j, \lambda_k \in \Lambda$.
- $S_{i,j} \in \mathbb{R}_+$: the data rate provisioned from ToRs i to j including both the direct connections through MEMS and indirect connections relayed at other ToRs, $i, j \in T, i \neq j$.
- $v_{i,j,k} \in \mathbb{R}_+$: the data rate from ToRs i to j through MEMS carried by wavelength λ_k, $i, j \in T, i \neq j, \lambda_k \in \Lambda$.

The MILP formulation of the optical network configuration in Proteus is expressed as [70]

$$\text{maximize} \quad \sum_{\substack{i,j \in T \\ i \neq j}} S_{i,j} \tag{5.3}$$

$$\text{subject to} \quad w_{i,j,k} \leq l_{i,j}, \qquad \forall i, j \in T, i \neq j, \lambda_k \in \Lambda, \tag{5.4}$$

$$\sum_{\substack{j \in T \\ j \neq i}} w_{j,i,k} \leq 1, \qquad \forall i \in T, \lambda_k \in \Lambda, \tag{5.5}$$

$$\sum_{\substack{j \in T \\ j \neq i}} w_{i,j,k} \leq 1, \qquad \forall i \in T, \lambda_k \in \Lambda, \tag{5.6}$$

$$\sum_{\substack{j\in T\\ j\neq i}} l_{i,j} = W, \qquad \forall i \in T, \tag{5.7}$$

$$v_{i,j,k} \leq \min\{C_{\text{port}}, C_\lambda \times w_{i,j,k}\}, \qquad \forall i,j \in T, i \neq j, \lambda_k \in \Lambda, \tag{5.8}$$

$$S_{i,j} \leq D_{i,j}, \qquad \forall i,j \in T, i \neq j, \tag{5.9}$$

$$\sum_{\substack{j\in T\\ j\neq i}} \sum_{\lambda_k\in\Lambda} v_{i,j,k} - \sum_{\substack{j\in T\\ j\neq i}} S_{i,j} = \sum_{\substack{j\in T\\ j\neq i}} \sum_{\lambda_k\in\Lambda} v_{j,i,k} - \sum_{\substack{j\in T\\ j\neq i}} S_{j,i}, \qquad \forall i \in T. \tag{5.10}$$

Objective (5.3) maximizes the total provisioned throughput in Proteus. Constraint (5.4) imposes that a wavelength λ_k can only be used between one pair of ToRs if they are connected through the MEMS. Constraints (5.5) and (5.6) state that each ToR can use one wavelength to connect to at most one ToR. Constraint (5.7) ensures that the number of connections established per ToR is limited by the number of ports in the WSS. Constraint (5.8) imposes an upper bound on the data rate for connections through MEMS. Constraint (5.9) states that we never provision more data rate than needed. Equation (5.10) is the flow conservation constraint, i.e., the outgoing transit traffic equals incoming transit traffic at each ToR.

5.3.3 Resource Allocation in SDM-Based DCNs

The SDM-based DCN architecture shown in Fig. 5.5 has a relatively simple topology, where routes of all the traffic demands are already fixed and only spectral and spatial elements need to be assigned. For the different SDM switching schemes introduced in Section 5.2.4, the formation of spectral–spatial connections are similar but their levels of flexibilities in utilizing resources are different. In [Paper E], both optimization formulations and heuristics are studied for these SDM switching schemes.

Another worth noting issue in SDM-based DCNs is the performance trade-off between throughput maximization and blocking probability minimization caused by unbalanced distribution of data rates. It has been shown that the majority of flows within DCNs have low data rates (the so-called mice flows), yet the majority of throughput belongs to a few "elephant flows" [25–28]. This unbalance becomes more severe when traffic demands are aggregated in MDCs. Consequently, the minimization of blocking probability may give rise to high blocking of bandwidth-intensive connections and reduce the total throughput. On the other hand, maximizing the throughput may lead to blocking of an excessive number of low-data-rate flows. This performance trade-off is identified and studied in [Paper E], where the two metrics are combined linearly by a weight factor in resource allocation. By tuning the weight factor, the best balance between the throughput and blocking probability can be achieved.

Chapter 6

Contributions

This chapter summarizes the contributions of the appended papers.

Paper A

"Link-Level Resource Allocation for Flexible-Grid Nonliear Fiber-Optic Communication Systems"

In this paper, we propose an optimization formulation to allocate the transmission parameters of all the traffic demands in a single flexible-grid link. The GN model is used in our algorithm to accurately predict the connection QoTs. Compared with a simpler algorithm based on transmission reach, the GN model based optimization can flexibly adjust the connection spacings and modulation formats such that the overall spectrum usage of the system is significantly reduced. In the single link scenario, the spectrum usage is demonstrated insensitive to the spectral ordering of traffic demands.

Contributions: LY performed mathematical modelling, numerical calculations, and data analysis of the resource allocation problem and wrote the paper. EA and HW contributed to result presentation. PJ provided advices on the GN model. RDT and MBP gave feedback on paper writing. All authors reviewed and revised the paper.

Context: the GN model is discussed in Section 2.6 and the resource allocation is related to Section 3.5.

Paper B

"Resource Allocation for Flexible-Grid Optical Networks With Nonlinear Channel Model"

This paper generalizes the method in Paper A to network-level optimization of transmission parameters. The PSD, modulation format, and carrier frequency of each individual traffic demand are optimized to minimize the spectrum usage and maximize the overall

SNR margins. The effectiveness of the proposed algorithm is demonstrated in various network scenarios. We also analyze the relation between modulation formats and transmission distance based on the results of the proposed method.

Contributions: LY proposed the optimization formulation, performed simulations, and wrote the paper. EA, HW, and MBP contributed to the analysis and provided mathematical expertise. All authors reviewed and revised the paper.

Context: Section 3.5.

Paper C

"Joint Assignment of Power, Routing, and Spectrum in Static Flexible-Grid Networks"

In Paper B, we assume that the routes and spectrum orderings of traffic demands are precalculated. In this paper, we develop an MILP to incorporate the routing and spectrum assignment into the resource allocation algorithm. Moreover, the PSD of individual traffic demands is also optimized to mitigate the NLI between optical connections. To make the problem numerically tractable, the nonlinear expressions in the GN model are linearized by piecewise linear functions and included into the MILP to describe QoTs. Low complexity heuristic algorithms are also proposed to solve the resource allocation problem.

Contributions: LY performed the optimization formulation, heuristic design, function linearization, and numerical simulations. EA contributed to the result analysis and presentation. MND and HW gave feedback on interpretation of the results. All authors reviewed and revised the paper.

Context: Section 3.5.

Paper D

"Robust Regenerator Allocation in Nonlinear Elastic Optical Networks With Time-Varying Data Rates"

In this paper, we investigate how to allocate regenerator sites robustly in optical networks when data rates of traffic demands are stochastic processes. The GN model and statistical network assessment process framework are used to characterize probabilistic distributions of PLIs for each demand, based on which a heuristic algorithm is proposed to select a set of regenerator sites with the minimum blocking probability. Our method achieves the same blocking probabilities with on average 10% less RSs compared with the method in Sections 4.3 and 4.4.

Contributions: LY formulated the problem, designed the algorithms, performed simulations and data analysis. YX and ND contributed to numerical calculations. MBP contributed to the problem formulation. EA provided suggestions on the result presentation. All authors reviewed and revised the paper.

Context: Section 4.5.

Paper E

"Network Performance Trade-Off in Modular Data Centers With Optical Spatial Division Multiplexing"

In this paper, we investigate the relation between the blocking and throughput in modular data center networks based on optical spatial division multiplexing. The two metrics are combined linearly by a weight factor that prioritizes them relatively. An effective heuristic algorithm is proposed for the resource allocation problem in three different spatial division multiplexing switching schemes. Simulation results demonstrate that carefully chosen weight factors are necessary to achieve a proper balance between the blocking probability and throughput in all the switching schemes.

Contributions: LY formulated the problem, designed the algorithms, performed simulations and data analysis. MF and AM provided mathematical expertise and background knowledge in DCNs. MT, EA, and LW contributed to the analysis and interpretation of the results. All authors reviewed and revised the paper.

Context: Sections 5.2 and 5.3.

References

[1] "Cisco visual networking index," Jun. 2014. [Online]. Available: http://www.cisco.com/c/en/us/solutions/service-provider/visual-networking-index-vni/index.html

[2] P. J. Winzer, "High-spectral-efficiency optical modulation formats," *IEEE Journal of Lightwave Technology*, vol. 30, no. 24, pp. 3824–3835, Dec. 2012.

[3] O. Gerstel, M. Jinno, A. Lord, and S. Yoo, "Elastic optical networking: A new dawn for the optical layer?" *IEEE Communications Magazine*, vol. 50, no. 2, pp. 12–20, Feb. 2012.

[4] *Spectral grids for WDM applications: DWDM frequency grid*, Telecommunication Standardization Sector of International Telecommunication Union Recommendation ITU-T G.694.1, Jun. 2012.

[5] A. Nag, M. Tornatore, and B. Mukherjee, "Optical network design with mixed line rates and multiple modulation formats," *IEEE Journal of Lightwave Technology*, vol. 28, no. 4, pp. 466–475, 2010.

[6] C. Laperle and K. Roberts, "Flexible transceivers," in *Proc. European Conference on Optical Communication (ECOC)*, Amsterdam, the Netherlands, Sept. 2012, p. We.3.A.3.

[7] D. Klonidis, F. Cugini, O. Gerstel, M. Jinno, V. Lopez, E. Palkopoulou, M. Sekiya, D. Siracusa, G. Thouénon, and C. Betoule, "Spectrally and spatially flexible optical network planning and operations," *IEEE Communications Magazine*, vol. 53, no. 2, pp. 69–78, Feb. 2015.

[8] M. Jinno, H. Takara, B. Kozicki, Y. Tsukishima, Y. Sone, and S. Matsuoka, "Spectrum-efficient and scalable elastic optical path network: Architecture, benefits, and enabling technologies," *IEEE Communications Magazine*, vol. 47, no. 11, pp. 66–73, Nov. 2009.

[9] P. Johannisson and E. Agrell, "Modeling of nonlinear signal distortion in fiber-optic networks," *IEEE Journal of Lightwave Technology*, vol. 32, no. 23, pp. 3942–3950, 2014.

[10] P. Johannisson and M. Karlsson, "Perturbation analysis of nonlinear propagation in a strongly dispersive optical communication system," *IEEE Journal of Lightwave Technology*, vol. 31, no. 8, pp. 1273–1282, Oct. 2013.

[11] A. Splett, C. Kurtzke, and K. Petermann, "Ultimate transmission capacity of amplified optical fiber communication systems taking into account fiber nonlinearities," in *Proc. European Conference and Exhibition on Optical Communication (ECOC)*, Montreux, Switzerland, Sept. 1993, p. MoC2.4.

[12] P. Poggiolini, "The GN model of non-linear propagation in uncompensated coherent optical systems," *IEEE Journal of Lightwave Technology*, vol. 30, no. 24, pp. 3857–3879, Dec. 2012.

[13] A. Carena, V. Curri, G. Bosco, P. Poggiolini, and F. Forghieri, "Modeling of the impact of nonlinear propagation effects in uncompensated optical coherent transmission links," *IEEE Journal of Lightwave Technology*, vol. 30, no. 10, pp. 1524–1539, Apr. 2012.

[14] P. Poggiolini, G. Bosco, A. Carena, V. Curri, Y. Jiang, and F. Forghieri, "The GN-model of fiber non-linear propagation and its applications," *IEEE Journal of Lightwave Technology*, vol. 32, no. 4, pp. 694–721, Jan. 2014.

[15] B. G. Bathula, R. K. Sinha, A. L. Chiu, M. D. Feuer, G. Li, S. L. Woodward, W. Zhang, R. Doverspike, P. Magill, and K. Bergman, "Constraint routing and regenerator site concentration in ROADM networks," *IEEE/OSA Journal of Optical Communications and Networking*, vol. 5, no. 11, pp. 1202–1214, Oct. 2013.

[16] B. G. Bathula, A. L. Chiu, R. K. Sinha, and S. L. Woodward, "Routing and regenerator planning in a carrier's core ROADM network," in *Proc. Optical Fiber Communication Conference (OFC)*, Los Angeles, CA, Mar. 2017, pp. Th4F–4.

[17] F. Kuipers, A. Beshir, A. Orda, and P. Van Mieghem, "Impairment-aware path selection and regenerator placement in translucent optical networks," in *Proc. International Conference on Network Protocols (ICNP)*, Kyoto, Japan, Oct. 2010, pp. 11–20.

[18] S. Varma and J. P. Jue, "Regenerator placement and waveband routing in optical networks with impairment constraints," in *Proc. International Conference on Communications (ICC)*, Kyoto, Japan, Jul. 2011, pp. ONSP–1.

[19] J. Pedro, "Predeployment of regenerators for fast service provisioning in DWDM transport networks," *IEEE/OSA Journal of Optical Communications and Networking*, vol. 7, no. 2, pp. A190–A199, Nov. 2015.

[20] S. Varma and J. P. Jue, "Regenerator site selection in mixed line rate waveband optical networks," *IEEE/OSA Journal of Optical Communications and Networking*, vol. 5, no. 3, pp. 198–209, Mar. 2013.

[21] W. Xie, J. P. Jue, X. Wang, Q. Zhang, Q. She, P. Palacharla, and M. Sekiya, "Regenerator site selection for mixed line rate optical networks," *IEEE/OSA Journal of Optical Communications and Networking*, vol. 6, no. 3, pp. 291–302, Feb. 2014.

[22] Y. Liu, H. Yuan, A. Peters, and G. Zervas, "Comparison of SDM and WDM on direct and indirect optical data center networks," in *Proc. European Conference on Optical Communication (ECOC)*, Düsseldorf, Germany, Sept. 2016, p. M.1.F.2.

[23] M. Fiorani, M. Tornatore, J. Chen, L. Wosinska, and B. Mukherjee, "Optical spatial division multiplexing for ultra-high-capacity modular data centers," in *Proc. Optical Fiber Communication Conference (OFC)*, Anaheim, CA, Mar. 2016, pp. Tu2H–2.

[24] ——, "Spatial division multiplexing for high capacity optical interconnects in modular data centers," *IEEE/OSA Journal of Optical Communications and Networking*, vol. 9, no. 2, pp. 143–153, Feb. 2017.

[25] A. Greenberg, J. R. Hamilton, N. Jain, S. Kandula, C. Kim, P. Lahiri, D. A. Maltz, P. Patel, and S. Sengupta, "VL2: A scalable and flexible data center network," *ACM Computer Communication Review*, vol. 39, no. 4, pp. 51–62, Aug. 2009.

[26] T. Benson, A. Anand, A. Akella, and M. Zhang, "Understanding data center traffic characteristics," *ACM Computer Communication Review*, vol. 40, no. 1, pp. 92–99, Jan. 2010.

[27] T. Benson, A. Akella, and D. A. Maltz, "Network traffic characteristics of data centers in the wild," in *Proc. Internet Measurement Conference*, Melbourne, Australia, Nov. 2010, pp. 267–280.

[28] A. Roy, H. Zeng, J. Bagga, G. Porter, and A. C. Snoeren, "Inside the social network's (datacenter) network," *ACM Computer Communication Review*, vol. 45, no. 4, pp. 123–137, Aug. 2015.

[29] V. López and L. Velasco, *Elastic Optical Networks: Architectures, Technologies, and Control*. Springer, 2016.

[30] Y. Pointurier, "Design of low-margin optical networks," *IEEE/OSA Journal of Optical Communications and Networking*, vol. 9, no. 1, pp. A9–A17, 2017.

[31] G. P. Agrawal, *Nonlinear fiber optics*. Academic Press, Dec. 2006.

[32] ——, *Fiber-optic communication systems*. John Wiley & Sons, Feb. 2002.

[33] E. Ip and J. M. Kahn, "Compensation of dispersion and nonlinear impairments using digital backpropagation," *IEEE Journal of Lightwave Technology*, vol. 26, no. 20, pp. 3416–3425, Dec. 2008.

[34] N. Irukulapati, H. Wymeersch, P. Johannisson, and E. Agrell, "Stochastic digital backpropagation," *IEEE Transactions on Communications*, vol. 62, no. 11, pp. 3956–3968, Nov. 2014.

[35] R. J. Essiambre and P. J. Winzer, "Fibre nonlinearities in electronically pre-distorted transmission," p. Tu3.2.2, Sept. 2005.

[36] D. J. Ives and S. J. Savory, "Transmitter optimized optical networks," in *Proc. Optical Fiber Communication Conference (OFC)*, Anaheim, CA, Mar. 2013, p. JW2A.64.

[37] K. Christodoulopoulos, K. Manousakis, and E. Varvarigos, "Reach adapting algorithms for mixed line rate WDM transport networks," *IEEE Journal of Lightwave Technology*, vol. 29, no. 21, pp. 3350–3363, Nov. 2011.

[38] A. Klekamp, R. Dischler, and F. Buchali, "Limits of spectral efficiency and transmission reach of optical-OFDM superchannels for adaptive networks," *IEEE Photonics Technology Letters*, vol. 23, no. 20, pp. 1526–1528, Jul. 2011.

[39] K. Cho and D. Yoon, "On the general BER expression of one-and two-dimensional amplitude modulations," *IEEE Transactions on Communications*, vol. 50, no. 7, pp. 1074–1080, Nov. 2002.

[40] P. K. Vitthaladevuni, M.-S. Alouini, and J. C. Kieffer, "Exact BER computation for cross QAM constellations," *IEEE Transactions on Wireless Communications*, vol. 4, no. 6, pp. 3039–3050, Dec. 2005.

[41] J. M. Simmons, *Optical network design and planning.* Springer, 2014.

[42] E. Agrell, M. Karlsson, A. Chraplyvy, D. J. Richardson, P. M. Krummrich, P. Winzer, K. Roberts, J. K. Fischer, S. J. Savory, B. J. Eggleton *et al.*, "Roadmap of optical communications," *Journal of Optics*, vol. 18, no. 6, p. 063002, 2016.

[43] G. N. Rouskas and H. G. Perros, "A tutorial on optical networks," *Advanced Lectures on Networking*, pp. 155–193, Nov. 2002.

[44] R. Ramaswami, K. Sivarajan, and G. Sasaki, *Optical networks: A practical perspective.* Morgan Kaufmann, Aug. 2009.

[45] Z. Liu and G. N. Rouskas, "Link selection algorithms for link-based ILPs and applications to RWA in mesh networks," in *Proc. International Conference of Optical Network Design and Modeling (ONDM)*, Brest, France, Apr. 2013, pp. 59–64.

[46] K. Christodoulopoulos, K. Manousakis, and E. Varvarigos, "Offline routing and wavelength assignment in transparent WDM networks," *IEEE Transactions on Networking*, vol. 18, no. 5, pp. 1557–1570, Oct. 2010.

[47] D. J. Ives, P. Bayvel, and S. J. Savory, "Physical layer transmitter and routing optimization to maximize the traffic throughput of a nonlinear optical mesh network," in *Proc. International Conference of Optical Network Design and Modeling (ONDM)*, Stockholm, Sweden, May 2014, pp. 168–173.

[48] J. Y. Yen, "Finding the k shortest loopless paths in a network," *Management Science*, vol. 17, no. 11, pp. 712–716, Jul. 1971.

[49] K. Christodoulopoulos, I. Tomkos, and E. Varvarigos, "Elastic bandwidth allocation in flexible OFDM-based optical networks," *IEEE Journal of Lightwave Technology*, vol. 29, no. 9, pp. 1354–1366, May 2011.

[50] S. Talebi, F. Alam, I. Katib, M. Khamis, R. Salama, and G. N. Rouskas, "Spectrum management techniques for elastic optical networks: A survey," *Optical Switching and Networking*, vol. 13, pp. 34–48, Feb. 2014.

[51] B. C. Chatterjee, N. Sarma, and E. Oki, "Routing and spectrum allocation in elastic optical networks: A tutorial," *IEEE Communications Surveys & Tutorials*, vol. 17, no. 3, pp. 1776–1800, May 2015.

[52] J. Zhao, H. Wymeersch, and E. Agrell, "Nonlinear impairment-aware static resource allocation in elastic optical networks," *IEEE Journal of Lightwave Technology*, vol. 33, no. 22, pp. 4554–4564, Nov. 2015.

[53] P. Poggiolini, G. Bosco, A. Carena, R. Cigliutti, V. Curri, F. Forghieri, R. Pastorelli, and S. Piciaccia, "The LOGON strategy for low-complexity control plane implementation in new-generation flexible networks," in *Proc. Optical Fiber Communication Conference (OFC)*, Anaheim, CA, Mar. 2013, p. OW1H.3.

[54] R. Pastorelli, "Network optimization strategies and control plane impacts," in *Proc. Optical Fiber Communication Conference (OFC)*, Los Angeles, CA, Mar. 2015, p. M2I.6.

[55] Optelian Access Networks Corporation, "Transponders and regenerators data sheet," Jan. 2017. [Online]. Available: https://www.optelian.com/wp-content/uploads/2017/02/Optelian-TranspondersRegenerators-DS-0117.pdf

[56] Oclaro, Inc., "OTS-4400 DPSK regenerator," Aug. 2014. [Online]. Available: http://www.oclaro.com/wp-content/uploads/2014/08/3010006-00-OTS-4400-DPSK-Data-Sheet-091612.pdf

[57] W. Zhang, J. Tang, K. E. Nygard, and C. Wang, "REPARE: Regenerator placement and routing establishment in translucent networks," in *Proc. Global Telecommunications Conference (GLOBECOM)*, Honolulu, HI, Dec. 2009, pp. 1–7.

[58] M. Klinkowski, M. Ruiz, L. Velasco, D. Careglio, V. Lopez, and J. Comellas, "Elastic spectrum allocation for time-varying traffic in flexgrid optical networks," *Journal on Selected Areas in Communications*, vol. 31, no. 1, pp. 26–38, 2013.

[59] A. Asensio, M. Klinkowski, M. Ruiz, V. López, A. Castro, L. Velasco, and J. Comellas, "Impact of aggregation level on the performance of dynamic lightpath adaptation under time-varying traffic," in *Proc. IEEE International Conference of Optical Network Design and Modeling (ONDM)*, Brest, France, Apr. 2013, pp. 184–189.

[60] F. Paolucci, A. Castro, F. Fresi, M. Imran, A. Giorgetti, B. B. Bhownik, G. Berrettini, G. Meloni, F. Cugini, L. Velasco *et al.*, "Active PCE demonstration performing elastic operations and hitless defragmentation in flexible grid optical networks," *Photonic Network Communications*, vol. 29, no. 1, pp. 57–66, 2015.

[61] M. Cantono, R. Gaudino, and V. Curri, "Potentialities and criticalities of flexible-rate transponders in DWDM networks: A statistical approach," *IEEE/OSA Journal of Optical Communications and Networking*, vol. 8, no. 7, pp. A76–A85, 2016.

[62] V. Curri, M. Cantono, and R. Gaudino, "Elastic all-optical networks: A new paradigm enabled by the physical layer. How to optimize network performances?" *IEEE Journal of Lightwave Technology*, vol. 35, no. 6, pp. 1211–1221, 2017.

[63] M. F. Habib, M. Tornatore, M. De Leenheer, F. Dikbiyik, and B. Mukherjee, "Design of disaster-resilient optical datacenter networks," *IEEE Journal of Lightwave Technology*, vol. 30, no. 16, pp. 2563–2573, Aug. 2012.

[64] C. Kachris and I. Tomkos, "A survey on optical interconnects for data centers," *IEEE Communications Surveys and Tutorials*, vol. 14, no. 4, pp. 1021–1036, Jan. 2012.

[65] M. Al-Fares, A. Loukissas, and A. Vahdat, "A scalable, commodity data center network architecture," *ACM SIGCOMM Computer Communication Review*, vol. 38, no. 4, pp. 63–74, Aug. 2008.

[66] T. Chen, X. Gao, and G. Chen, "The features, hardware, and architectures of data center networks: A survey," *Journal of Parallel and Distributed Computing*, vol. 96, pp. 45–74, Oct. 2016.

[67] "HP helps customers manage business growth with compact, shipped-to-order data centers," Jul. 2008. [Online]. Available: http://www.hp.com/hpinfo/newsroom/press/2008/080716xa.html

[68] G. Wang, D. G. Andersen, M. Kaminsky, K. Papagiannaki, T. Ng, M. Kozuch, and M. Ryan, "C-Through: Part-time optics in data centers," *ACM SIGCOMM Computer Communication Review*, vol. 40, no. 4, pp. 327–338, Aug. 2010.

[69] N. Farrington, G. Porter, S. Radhakrishnan, H. H. Bazzaz, V. Subramanya, Y. Fainman, G. Papen, and A. Vahdat, "Helios: A hybrid electrical/optical switch architecture for modular data centers," *ACM Computer Communication Review*, vol. 40, no. 4, pp. 339–350, Aug. 2010.

[70] A. Singla, A. Singh, K. Ramachandran, L. Xu, and Y. Zhang, "Proteus: A topology malleable data center network," in *Proceedings of ACM SIGCOMM Workshop on Hot Topics in Networks*, Monterey, CA, Oct. 2010, pp. 8:1–8:6.

[71] D. Richardson, J. Fini, and L. Nelson, "Space-division multiplexing in optical fibres," *Nature Photonics*, vol. 7, no. 5, pp. 354–362, 2013.

[72] J. Edmonds, "Paths, trees, and flowers," *Canadian Journal of Mathematics*, vol. 17, no. 3, pp. 449–467, Feb. 1965.

[73] V. Kolmogorov, "Blossom V: A new implementation of a minimum cost perfect matching algorithm," *Mathematical Programming Computation*, vol. 1, no. 1, pp. 43–67, 2009.